REPORT DOCUMENTATION PAGE

Form Approved OMB No. 0704-0188

Public reporting burden for this collection of information is estimated to average 1 hour per response, including the time for reviewing instructions, searching existing data sources, gathering and maintaining the data needed, and completing and reviewing the collection of information. Send comments regarding this burden estimate or any other aspect of this collection of information, including suggestions for reducing this burden to Washington Headquarters Services, Directorate for Information Operations and Reports, 1215 Jefferson Davis Highway, Suite 1204, Arlington, VA 22202-4302, and to the Office of Management and Budget, Paperwork Reduction Project (0704-0188), Washington, DC 20503.

1. AGENCY USE ONLY (Leave blank)	2. REPORT DATE	3. REPORT TYPE AND DATES COVERED
	January 1995	Final Report

4. TITLE AND SUBTITLE

A Study of Characteristics of Seismic Wave Propagation in the Lithosphere of Northern Eurasia Using GEON and Other Long Range Profiles and to Develop Methods of Dynamic Imaging of the Deep Seismic Sounding 2-D Models

5. FUNDING NUMBERS

F6170894W0790

6. AUTHOR(S)

Dr. Nina Pavlenkova

7. PERFORMING ORGANIZATION NAME(S) AND ADDRESS(ES)

Institute for Physic of the Earth
Bolshaya Gruzhimskaya Ul.
Bldg No 10
Moscow 123810
Russia

8. PERFORMING ORGANIZATION REPORT NUMBER

N/A

9. SPONSORING/MONITORING AGENCY NAME(S) AND ADDRESS(ES)

EOARD
PSC 802 BOX 14
FPO 09499-0200

10. SPONSORING/MONITORING AGENCY REPORT NUMBER

SPC 94-4083

11. SUPPLEMENTARY NOTES

12a. DISTRIBUTION/AVAILABILITY STATEMENT

Approved for public release; distribution is unlimited.

12b. DISTRIBUTION CODE

A

13. ABSTRACT (Maximum 200 words)

This report results from a contract tasking Institute for Physic of the Earth as follows: Study characteristics of seismic wave propagation in the lithosphere of northern Eurasia using GEON and other long range profiles.

14. SUBJECT TERMS

EOARD

15. NUMBER OF PAGES

55

16. PRICE CODE

N/A

17. SECURITY CLASSIFICATION OF REPORT	18. SECURITY CLASSIFICATION OF THIS PAGE	19, SECURITY CLASSIFICATION OF ABSTRACT	20. LIMITATION OF ABSTRACT
UNCLASSIFIED	UNCLASSIFIED	UNCLASSIFIED	UL

NSN 7540-01-280-5500

Standard Form 298 (Rev. 2-89)
Prescribed by ANSI Std. 239-18
298-102

19990203 040

Ref: SPC -94-4083

FINAL REPORT

for the special contract SPC-94-4083

Principal Investigator (PI) Name and Address:
Pavlenkova Ninel Ivanovna
Institute for Physics of the Earth
123810 Moscow, ul.B.Grusinskaja 10
Russia

Dates of Contract : January 1, 1994 - December 31,1994

Primary objectives and scope of the project.

The contructers planed to study characteristics of seismic wave propagation in the lithosphere of Northern Eurasia using GEON and other long range profiles and to develop methods of dynamic imaging of the deep seismic sounding 2-D models.

Summary of Completed Work.

Long-range seismic studies made by Russian institutions during the last two decades reached the depths of 700-800 km (Peace Nuclear Explosions were used as a source) . Comparison of the wave-fields from these and other seismic profiles in Russia, West Europe and the South Atlantic showed that the uppermost mantle including the thermal lithosphere and asthenosphere is characterised by fine stratification: high velocities (up to 8.6 km/s) alternate with lower ones (7.8-8.0 km/s). A rheologically weak layer underlain by a seismic boundary of global significance is distinguished at a depth of 80-100 km. It is located inside the thermal lithosphere beneath old platforms and at the bottom of the lithosphere beneath active tectonic areas. A change of velocity pattern where the block structure of the uppermost mantle is transformed into a horizontally homogeneous one, and a local isostatic equilibrium are typical at the boundary. These features suggest that the boundary separates the brittle and more ductile upper mantle layers and that it may be considered as the bottom of the global mechanical lithosphere.

. Beneath the western part of the Siberian Craton two blocks with anomalously high velocities (8.5-8.6 km/s) were outlined . The observed gravity, magnetic and heat flow fields do not correlate with the high velocity blocks. Assuming that normal uppermost mantle velocities can not be higher then 8.3-8.4 km/s the observed anomalous high values may be considered as an effect of velocity anisotropy but an azimuthal one because the high velocities are observed in crossed profiles.

An attempt was made to apply the migration technique to ridely spaced and low-fold wave field data as the ordinary wide-angle reflection data. The migration method, developed by V.N. Pilipenko and based on finite-difference solutions of the time and wave equations on the special grids was applied. Specific feature of the method is a special transformation of the grids for different types of waves. The 'Polar profile' in Northern Scandinavia, was chosen for the proceeding. The results show perspective of the migration but more dense observations are needed. On some noise background formed by the migration 'smiles', many specific features of the Moho structure clearly observed beneath the tectonic units of different ages. An impressive feature of the migrated cross-sections is also the boundary at a depth of 35 km in the Proterozoic block which is well traced in the P-wave field and does not exist in the S-wave field. A correspondent change of the P- and S velocity ratio beneath this boundary is also observed.

1. Introduction

The contract suggested the study of characteristics of seismic wave propagation in the lithosphere of the Northern Eurasia. It was based on the seismic data obtained on the long-range profiles in the territory of

DTIC QUALITY INSPECTED 2

AQF 99-05-0837

the former USSR (DSS data) and inWest Europe. The largest part of the data covered the USSR, because they have not be studied before in details , where as the data from Western Europe and other regions were used mostly for comparison.

Considerable progress in the studies was attributed to the activities of GEON Centre of the former Ministry of Geology of USSR. GEON covered almost the whole territory of the USSR with a regular network of profiles (Fig.1) coupled with seismic research, which included 3-component magnetic recordings of shots of different strength at a large number of stations (up to 300) positioned on profiles 2500-3000 km long (Benz et.al., 1992).. Special low-frequency seismic stations were constructed for this studies. Two types of sources were used; the first type were chemical explosions with up to 5000 kg loads in holes spaced 100-150 km apart. They allowed recordings at distances of 300-400 km. The second type were Peace Nuclear Explosions (PNE) specially made for this research. Two to four such shots were made on several profiles, as a result, these seismic profiles are unique on the global basis. The data were confidential for a long time and their interpretation in form of the mantle models were made only for some profiles: "Craton", "Kimberlite" (Yegorkin @ Pavlenkova,1981, Egorkin @ Chernyshov, 1983, Pavlenkova @ Yegorkin, 1983, Egorkin et.al., 1987). Now some international groups are working on the data from "Rift" and "Quarts" profiles (Mechie et.al., 1993, Cipar et.al., 1993, Priestly et.al., 1994). This contract suggested interpretation the data from the "Rift" and "Meteorite" profiles in form of 2-D models and comprehensive analysis of all seismic data obtained on the continent.

These contract studies were going in three directions and three groups of investigators were involved in the study:

Group 1 worked in the Institute for Physics of the Earth of the Russian Academy of Science and was headed by Nina Pavlenkova. It dealt mainly with comparative analysis of the mantle wave fields for all existing in the North Eurasia seismic profiles to determine the principal features of the upper mantle stratification and general features of the mantle wave fields.

Group II worked in GEON Centre and was headed by L.Solodilov and Galina Pavlenkova. They made interpretation of the data on the upper mantle structure of the Siberian Craton, construction 2D models along the profiles "Rift" and "Meteorite".

Group III worked at the Institute of Geophysics of the Ukrainian Academy of Science, Kiev, in co-operation with Institute of Physics of the Earth. It was headed by V.Pilipenko and Nina Pavlenkova. They carried out comparative analysis of the crustal P- and S- wave velocities and their dependence on geological structure of the
Baltic Shields and studies of the crustal boundary characteristics by means of the wide-angle reflection migration.

The main results of these three groups studies are presented in the next three sections.

I. GENERAL FEATURES OF THE OBSERVED WAVE FIELDS AND THE UPPER MANTLE STRATIFICATION.

To determine general features of the upper mantle wave fields and a generalised upper mantle model of the Northern Eurasia all observed data (record-sections, travel-times and amplitudes of mantle waves) from GEON profiles were used. A similar analysis will be made for the long-range profiles with mantle waves in Western Europe.

The previous upper mantle studies have shown a complicated velocity structure with many sharp boundaries and thin, alternating low and high velocity layers (Ansorge et al.,1979, Mueller and Ansorge, 1988, Prodehl, 1984, Guggisberg et al.,1991). Some correlation were determined between these inhomogeneities and thermal regimes, ages of structures and gross tectonic features (Fuchs, 1983, Pavlenkova and Yegorkin, 1983, Fuchs and Froidevaux, 1987). However the correlation are very often

difficult to observe because regional or global features of the upper mantle velocity structure are sometimes lost in the background of random distribution of strong local heterogeneities.

As a result many important questions remain unresolved. For instance:

- are there global discontinuities and some characteristic layering in the upper mantle or are the observed seismic boundaries and other inhomogeneities of short wavelength and randomly distributed in space?
- is there a continuous asthenosphere underlying the lithosphere or is it a group of asthenospheric lenses located at different depths?

We made an attempt to answer these questions analysing the PNE' records. They have provided recording to 3000 km which allow us to image the mantle to depths of 600-700 km.. These data have increased the resolving power of the seismological methods and they are more susceptible to lateral and vertical heterogeneity. The major attention we paid to identification the wave field features common to many regions that has important emphasizings regarding global upper mantle structure. Two regions with the deepest DSS studies were chosen for such comparison, Russia and West Europe, and than the results from these regions were compared with other regions including the ocean - Angola-Brazil Geotraverse.

a.. General features of the upper mantle waves in Russia.

To find some general features of the upper mantle structure, the wave fields were compared for all existing profiles (Fig.1). In Figures 2-9 typical record sections, travel-time curves and amplitude plots of mantle waves are presented. They show that in spite of the observed variations in the travel times and differences in apparent velocities some regular features of the wave fields and some principal wave groups may be distinguished.

As follows from the record sections (Fig.2-5) the upper mantle waves fall into two basic groups, "a" and "b" with essentially different apparent velocities. The registration interval for wave group "a" is 200-2000 km, and the apparent velocity changes within a wide range of 7.8-8.6 km/s. The wave group "b" composes secondary arrivals at distances of 1600-2300 km with apparent velocities of 9,5-10.5 km/s and the first arrivals traced at a distance of 2300-3000 km with average velocities 10.5-11.5 km/s. These waves are well known in seismology. The bend of their travel-time curves at 2300 km from the source is associated with the transition zone from the upper to the lower mantle at depth of 400-700 km.

The group “a” is composed from several waves (Fig.8). The first wave is designated P_n . The observed distance for this wave is 200-700 km and depths of ray penetration are 50-80 km. Its amplitude attenuates rather sharply with distance (mean attenuation coefficient a = 0.003-0.045 km). Apparent velocities of these waves are particularly variable, being from 7.8 to 8.6 km/s. As 3-D ray tracing showed (Matveeva and Pavlenkova, 1983), this variability of the refraction first arrivals could not be caused by three dimensional wave propagation. Only secondary arrivals formed mainly by the reflections, may be effected by so-called ‘side’ waves. The observed P_n velocities show a real complicated block structure of the mantle beneath the M boundary.

The next wave (P_N) is recorded as first arrivals at epicentral distances of 800-1500 km and is detected by a slight bend in the travel-time curve, when the dominant average velocities of 8.2-8.4 km/s change to 8.4-8.6 km/s (Fig.4). This wave is often observed as second arrivals as well (Fig.6,7). It is typically a complex group of phases suggesting the existence of a complicated boundary at a depth of around 100-110 km (we called it as the N boundary but maybe it correspond to the H discontinuity determined by A.Hales (1969) from the earthquake seismology data. The travel times and velocities of this wave are more stable than those of P_n (Fig.8). In spite of the strong variation in P_n velocities, resulting in time differences for P_n arrivals of 4.0 sec, the P_N times differ for profiles large distances apart by in average 2.0 s. On the amplitude curves the P_N wave also lies in a region of practically constant intensity, which is evidence of its confinement to a layer with a vertical velocity gradient. Two types of

these two wave pattern are observed. For the normal velocities beneath the Moho (not more than 8.2 km/s) the P_n wave is recorded up to distances of 800-900 km where the P_N wave becomes the first arrivals (PNE C1 in Fig.2), while for the higher velocities the P_n wave attenuates at distances of 600-700 km and the time delay between the P_n and P_N waves reaches 2.0-3.0 sec (PNE M4 in Fig.5).

At distances of 1600-1800 km the first arrival amplitudes decrease and shadow zones are often observed up to 1900-2200 km (Fig.4,5,8).

In some cases before the shadow zone a new wave with apparent velocities around 8.7 km/s comes from the secondary arrivals (Fig.3,4). It is reflected or refracted at depths of around 200 km and maybe corresponds to the L boundary reported from seismological data (Andersen, 1989). Sometimes the secondary arrivals with apparent velocities of about 8.7 km/s are observed after the shadow zone ("Craton") or inside it ("Rift"). The travel time curves of these waves (marked by P_L in Fig.8) are not so tight as for the P_N waves: they differ by several seconds and can not belong to the same horizontal boundary. At present, it is difficult to say how regularly they are distributed in space, and for this a special study is necessary. However, it is clear that this group of waves reflects a layering in the thick zone at depths of 200-300 km and this zone is characterised in average by a small velocity gradient or by a velocity inversion.

The wave group "b" is also composed from several waves reflected and refracted from discontinuities at depth 410, 520 and 680 km (Fig.9). They are the most regular waves recorded at all profiles. The discontinuity at depth of 410 km (the top of the transition zone) is characterised with refraction P_{410} and reflections $P_{410}P$ recorded at the secondary arrivals at distances 1600-2200 km. They have great intensity and a low-frequency record (Figs.2-5). Apparent velocities of the refractions are around 10 km/s and of the reflections are 9.5 km/s. The discontinuities at depth 520 and 680 km generate usually only refractions with apparent velocities of 10.5 and 11.5 km/s. (Let us note that apparent velocities for all mantle waves are higher than the real ones because of Earth surface curvature. They are higher on 0.1-0.2 in the depth interval from 100 to 200 km and on 0.7-0.8 km/s at depth of 400-700 km). The interval of the wave P_{520} registration at the first arrivals is very short at the Siberian profiles (from 2300 to 2500 km) and differences in the observed velocities between the waves P_{520} and P_{680} are not so significant. However as follows from comparison of all travel time curves the wave P_{520} is observed on all profiles.

Thus, a comparison of wave patterns and travel-time curves of the principal waves for all reversed and overlapping profiles in Russia shows some regular features of the uppermost mantle wave pattern. The observed stability in the travel times, record distances, velocities and amplitudes of the principal wave groups may be considered as good arguments for suggesting some generalised features of North Eurasia upper mantle stratification.

Several principal layers may be determined in the model (Fig.10). They are characterised by the basic waves described. The first layer is determined at the depth interval from the Moho down to 80-100 km. Characteristic features of this layer arë a low velocity gradient which causes high attenuation of the Pn waves and an extreme velocity inhomogeneity. A strong horizontal changes of velocities from 8.0 to 8.6 km/s is characteristic for this layer.

The second layer is characterised by velocities of 8.4-8.5 km/s and by a higher vertical velocity gradient compared to the upper layer. Horizontally it is more homogeneous. This follows from the smaller variation of the P_N arrival times.

The N boundary dividing the two layers is not a simple sharp discontinuity. High amplitude and low attenuation of the waves from this boundary suggest a zone of alternating of high and low velocities or lamellae. Sometimes the phases from the individual lamellae can be distinguished and some local reflectors can also be determined. In some cases two waves from the top and the bottom of the lamellae

layer are observed construing its thickness to 10-20 km. A specific feature of the N boundary is also its location at the bottom of a zone of velocity inversion. Intensity of the inversion varies from one region to another and depends mainly on the velocity in the uppermost mantle (P_n velocity). If the latter is more than 8.3 km/s, the inversion before the N boundary is stronger. If the P_n wave velocity is normal (8.0-8.2 km/s), this inversion might be negligible.

The third layer with velocities 8.5-8.6 km/s is located at depths of 200 -400 km. Its structure is not clear now and need more studies because the depth interval from 200 to 400 km is very poor investigated by the seismic long-range profiles. The waves from these depths are not recorded at the first arrivals, it is a "hidden zone". Only some general remarks may be made about velocity structure of this layer. The shadow zone observed at distances 1700-2000 km suggests decreasing of the velocity gradient or a velocity inversion at depth around 200 km. At the top of this low velocity gradient zone and inside it there are several reflectors of the group L. They are traced at different depths in different regions and characterise local heterogeneity of the lower part of the upper mantle.

The next discontinuities which were revealed from the data are well known boundaries of the phase transition zones between the upper and lower mantle. It is outlined by three sharp boundaries with velocities 9.5 , 10.0 and 10.8 km/s. Their depths are around 410, 520 and 680 km.in the whole area under the discussion. It was clear from the observed travel times as well; the times of these waves are very close (Fig.9) for all explosions. High intensity of the waves corresponding to these boundaries suggests high velocity gradient in the layers between the boundaries.

b. The upper mantle structure in West Europe.

The long range profiles in West Europe are generally providing information only to depths of 100-120 km. The profiles were made at different times and have different quality of the mantle wave records. In Fig.11the records and the DSS lines are shown where waves were recorded from boundaries beneath the Moho.

The most known profile is the French profile (FP) - Bretaque- Provence (Hirn et al, 1973). Here for the first time the mantle waves could not be explained by a single wave because the P_n phase dies out beyond 210 km distance and the P_1 phase is seen between 310 and 540 km (Fig.11). To test the validity of this wave being a reflection from a boundary within the mantle a second profile was carried out which demonstrated that travel times of mantle phases vary with distance and not with station locations. This confirmed that the P_1 phase must be caused by upper mantle stratification rather than by near surface irregularities.

High quality mantle arrivals were also recorded on profiles along the Italian Peninsula between Puglia and Tuscany ((Morelli et al, 1977) and across the Provincial basin (Hirn et al.,1977). They showed attenuation of the P_n phases at distances of 150-200 km and intensive secondary arrivals at the larger distances (the waves E and P_1^N in Fig.11).

Additional information on the upper mantle propagation and structure were obtained during the European Geotraverse (EGT) Project. These records were obtained from the shot points (SP) A, B, D in the Corsica-Sardinia part of the EGT (Egger et al., 1988) and from SP's E and L in the Tunisia profiles (Res.group, 1992). In Fig.7a the mantle waves are marked by E and P_N . Similar waves were observed in the Iberian lithosphere (Mezena and Carreno, 1993).

Thus, the most pronounced feature of the mantle wave fields in all these profiles is their division into several branches which are often correlated as secondary arrivals with high amplitude. These waves suggest the subhorizontal layering of the uppermost mantle with alternation of high and low velocities . From the velocity models published at that time it was difficult to see if this stratification has some regional features, and if there are some layers or seismic boundaries more pronounced or more

significant than others. The models are difficult to compare because during their construction different assumptions were made about the thickness and intensity of the velocity inversions and as a result different depths to the same seismic boundaries might be obtained. In addition, as soon as the secondary arrivals were interpreted as reflections at the critical points, their apparent velocities were considered as the real ones and the boundaries with an unrealistically wide variation of velocities below them (from 8.5 to 9.4 km/s) were determined (Egger et al.,1988, Res.Group, 1992).

Our analysis of travel-times of all intensive secondary arrivals has however not shown large differences (Fig.12a). In contrary they have a good correlation. The branches marked by P_1, E, P_1^N form a single curve, which looks just like one reflection. They might correspond to the same near horizontal boundary at a depth around 90 km. In this study, if the depth is very close to the depth of the N boundary in Siberia, these waves were also named as P_N in Fig.12a and the corresponding boundaries as N. The velocities beneath these boundaries are difficult to determine because in many profiles only the reflections were recorded. But taking into account the dominant velocities at distances greater than 300-400 km they are thought to be no higher then 8.2-8.3 km/s.

The observed high apparent velocities of the waves P_1, E, P_1^N are due to their being recognised before the critical points. Due to the high intensity of these precritical reflections, we have to propose that in this region the N boundary is not a simple velocity discontinuity, but that it is probably a complicated zone with inner heterogeneity generating strong reflections before the critical points. A velocity inversion above the N boundary may be also suggested. It follows from the time delay observed between the P_n arrivals and the averaged travel time curve of the P_N reflections.

A complicated relationship is observed between the N boundary and the lithosphere-asthenosphere system in this region. The latter is characterised by strong changes of the heat flow and the lithosphere thickness. From surface wave data (Panza et al.,1980) the average depth to the asthenosphere is 90-100 km beneath West Europe but it uplifts up to 60 km in the Tyrrhenean Sea. The same depths are deduced from the heat flow data. Against such a background the depth of the N boundary looks surprisingly stable and independent of the temperature regime. In some areas it is located at the top of the asthenosphere, in others, inside it.

A better correlation is observed between the N boundary and the tomography data. As in Siberia, this boundary is located in the depth interval where the upper mantle structural pattern changes. The latter can be see in the tomography cross-section through the Tyrrhenean Sea (Spakman, 1988), where at the depth of around 100 km the high velocity inhomogeneities are replaced by the low velocity ones. Again it suggests that the N boundary is connected with a change in the rheological properties of the upper mantle. This suggestion is confirmed by the geoid anomaly interpretation along the EGT, which showed two possible levels of isostatic equilibrium, one at a depth of 150 km and the other at 80 km (Marquart and Lelgemann,1992).

All these data cover only upper 100 km of the mantle because the length of travel-time curves on the West European DSS profiles does not exceed 1000 km. The deeper part of the upper mantle can be studied there only from seismological data. The most important data from this view point are the records of the NORSAR array, which produce fine details, not only of the first but also of the secondary arrivals. To compare the data with Siberian long range profiles we have used records and travel-time curves given in papers by England et al. (1977), and by Grad (1987). The result of the comparison are given in Fig.13. The first travel-time curve in this figure is based on the records of the NORSAR array and on a network of other seismological stations in the south of Europe; the second travel time curve was derived from records of a nuclear test in East Europe. The difference in the travel-time inside the group for the western and eastern parts of the continent is around one second, the discrepancy in the averaged travel times for each group reaching large values.

The greatest differences between the European and Siberian travel times are in the wave group "a". Their travel-time curves for Western Europe normally lie higher than those for Eastern Europe by 1-2 s. The Siberian travel-times, at distances up to 1000 km, practically coincide with those for Eastern Europe, but at long distances (1000 - 2000 km) they are shorter (the time delay can be as large as 5 s). Fig.14 shows how the observed differences in the travel times looks in form of the velocity models of the upper mantle. It present a combine geophysical cross section along seismic profile from the North Atlantic to the Siberian Craton. The most essential structural differences are observed between western and eastern European blocks. The average value of the velocity in the uppermost 200 km of the mantle under Western Europe is 7.9-8.0 km/s; under the ancient platform it is 8.1-8.2 km/s. Moreover, at these depths the mantle is extremely heterogeneous since it contains numerous low velocity layers (up to 7.5 km/s).

The structure of the transition zone between the upper and lower mantle under Western Europe is also different. The reflections connected with top of this zone were not found here, whereas the first arrivals splits into several branches with different apparent velocities. This is evidence that the top of the transition zone in that region is not a sharp boundary, but a transition layer where velocity gradually changes with depth (Fig.14).

Thus, comparative analysis of the mantle wave fields for all existing in the North Eurasia seismic profiles allowed to determine the principal features of the upper mantle stratification. There are global discontinuities and some characteristic layering in the upper mantle which are common for different regions. The most interesting result is determination of the boundary at depths 80-100 km (the N boundary). It was determined at the same depth interval in very different tectonic regions: inside the lithosphere beneath the Siberian Craton and inside the asthenosphere or at the lithosphere-asthenosphere boundary beneath the young West-European plates. To understend the nature of this boundary let us consider some other geophysical data.

c. Nature of the N boundary

To determine the nature of the N boundary we analysed the seismic data from other regions including the oceanic ones, for instance, the Angola-Brazil Geotraverse. The latter represents the DSS studies that image the deepest portion of the oceanic lithosphere (Fig.15). The seismic observations using OBS's were carried out by the Institute for Physics of the Earth of the Russian Academy of Science (Pavlenkova et.al., 1993). Six long range seismic profiles, crossing major elements of the South Atlantic (Angola and Brazil basins and Mid-oceanic ridge), were shot along the Geotraverse. Recordings at distances up to 600 km were obtained on each profile, resulting in ray penetration to depth of 80-100 km. The OBS's located every 30-40 km along the profiles, recorded the 500 kg explosions shot in 3 to 5 km intervals along the profile.

Despite of the significant changes in the heat flow and gravity field along the Geotraverse, the recorded wave fields have many common features. In the mid-oceanic ridge and in the oceanic basins some regular wave groups are observed. They have similar apparent velocities of 8.4-8.6 km/s, but different time-distance registration intervals (Fig.16). The first group (P_n wave) is recorded at distances of 20-100 km and an intercept time (t_i) of 1-1.5 sec (the reduction velocity is 8.5 km/s and the correction for the water depth was made). Other groups were revealed: N_0 - at distances of 100-250 km and at t_i of around 3 sec, N_1 - at 200-400 km and 4 sec, and N_2 - at 300-600 km and 6-7 sec. The large amplitude N_0 wave was observed only in the middle part of the ridge and no deeper waves were recorded there. Two other wave groups were traced on all profiles of the Geotraverse. Usually time delays of 1.5-2.0 sec are observed between these two groups. Such a wave pattern is typical for a structure of alternating high and low velocity layers. The N_2 wave characteristics are similar to that of the N wave in West Europe:

they have the same interval of registration and similar apparent velocities (Fig.12), although the travel-time pattern of Pn waves (arrival times and velocities) differ in these two regions.

As a result of the wave field interpretation three boundaries separated by low velocity zones were determined in the upper mantle of the South Atlantic: N_0 at the depth of 35-40 km, N_1 at the depth of 40-50 km and N_2 at the depth of 80 km (Fig.15).

The most stable correlation is characteristic for the N_2 boundary. The waves from this boundary are stable in their arrival times, in their epicentral distances and in their highest amplitudes. From these characteristics the N_2 wave group is similar to the P_N wave in West Europe and Siberia. In both cases the boundary generating these waves is a complex heterogeneous zone overlain by a velocity inversion.

The same relationship as in West Europe is observed between the N_2 boundary and the lithosphere-asthenosphere system of the Atlantic. From the heat flow and the surface wave determinations the lithosphere thickness decreases from 60-70 km in the oceanic basins to 30-40 km in the ridge axis. This means that in the Angola and Brazil basins the N_2 boundary might be the bottom of the lithosphere but in the ridge area it is located inside the asthenosphere. The latter here does not look to be as a continuous low velocity body but a fir tree like set of asthenospheric lenses. Many other boundaries and low velocity layers characterise the oceanic lithosphere as well. The N_2 boundary is outstanding not only in the high intensity of its reflections and in its stability in depth. The isostatic equilibrium of the crust and the inhomogeneous uppermost mantle is observed at this boundary (Pavlenkova et.al.,1993).

The similar characteristic of the N boundary were observed in the Siberian craton. Such properties of the boundary as inner lamination, location at the bottom of the inversion zone and at the bottom of the horizontally inhomogeneous uppermost mantle also suggest that it is a boundary between a brittle part and a more ductile part of the upper mantle. The suggestion is confirmed by decreasing of the Q factor in the velocity inversion zones above the boundary (Egorkin and Kun, 1978) and by the observed isostatic equilibrium of the crust and the upper mantle at the N boundary level (Pavlenkova and Romanyuk, 1991). From this point of view the N boundary might be considered as the bottom of the lithosphere. However, according to the heat flow data, the lithosphere beneath the Siberian platforms is 200 km thick (Kutas and Smirnov,1991), and thus the N boundary is located within the lithosphere. The latter may be underlined here by .the boundary L observed at depths of 160-200 km.

The three considered regions are not the only areas where remarkable reflections and refractions have been recorded from a seismic discontinuity near 100 km depth. At this depth strong seismic boundaries were observed earlier in other regions as well. There are the controlled source explosion data obtained with refraction, wide-angle and near vertical reflection observations. The first records of the upper mantle reflections were got from the seismic profiles in Middle Asia (Ryaboy,1966). Multichannel observations with a station spacing of 100 m enable accurate correlation of secondary arrivals. Among them reflections from 80 km were traced continuously along the 1000 km profile Kapet-Dag - Aral Sea. In others areas of Middle Asia this boundary was also distinguished from converted waves. This boundary was also observed in the North America (Mueller and Ansorge, 1988, Benz and McCarthy,1994)

New data on the detailed layering in the uppermost mantle were obtained from CDP surveys (Posgay et al.,1988,). The most important of these surveys is the Skagerrak profile in Scandinavia. That reveals a transparent upper mantle in the depth range 30-60 km and a reflective zone at depth of 60-90 km. The most prominent reflections are from the base of the reflective zone at a depth of 90 km. It is a continuous and horizontal reflector, which can be referred to the N boundary (Lie et al., 1990).

Earthquake data also provide evidence for a discontinuity near 100 km depth. At first A.Hales distinguished it in Australia (Hales, 1969, Hales et.al., 1975), than it was found and called as H or G discontinuity in other regions (Revenaugh and Sipkin, 1991, Revenaugh and Jordan,1994). A zone of high seismic attenuation is also observed at a depth of 100 km which is considered as a global feature of the upper mantle (Jordan, 1981).

Thus, different seismic methods show clear uppermost mantle layering and a seismic boundary at a depth of around 100 km, which might have a global significance. The characteristic features of this boundary are the following:

1. The boundary depth range is a narrow interval (80-110 km) in different tectonic regions. The boundary is located inside the thermal lithosphere beneath the old platforms, at the bottom of the lithosphere beneath the active tectonic areas and occurs within the asthenosphere beneath the mid-oceanic ridges.
2. It is not a sharp discontinuity but a boundary layer with fine inner heterogeneity - a reflective zone with intense velocity inversions.
3. Relatively high velocities (8.4-8.5 km/s) are typical for the N boundary both in the old platforms and in the high heat flow oceanic areas.
4. A change of structure pattern, where the block structure of the uppermost mantle is transformed into a horizontally homogeneous one is typical at the boundary level.
5. An isostatic equilibrium is observed at this level as well.

The last two features suggest that the boundary separates the brittle and more ductile upper mantle layers.

The nature of the N boundary is difficult to explain in one simple way. In the high heat flow regions it might be refereed to partial melting at the depth of the observed low velocity layers. The horizontal variation of the low velocity zones and their correlation with heat flow and high conductivity zones (Gordienko and Pavlenkova, 1985) confirm their connection with the melting areas. A similar explanation of the 100 km mantle boundaries has been done by Lie at.al.(1990) who considered "a model consisting of the mechanically strong upper lithosphere, underlain by a thermal boundary layer which separates it from the convecting asthenosphere". The presence of shear strain may also favor layers with oriented olivine. The latter can explain the observed high velocities due to the anisotropy . However, the partial melting cannot explain the N boundary location at similar depths in different temperature regimes and inside the lithosphere beneath the Siberian Craton. But it is difficult to propose that the common features of the wave fields in the South Atlantic, West Europe and the central areas of Eurasia are fortuitous. It is more realistic to propose that the depth of 80-100 km is a critical depth in the upper mantle where some global changes of matter occur. Hales et.al.(1975) interpreted the 100 km depth discontinuity as a phase transition from spinel to garnet peridotite. Petrological data suggest, however, that the boundary can not be related to a large-scale compositional change or to a global-scale mineralogical phase change (Sobolev and Fuchs,1993, Yu.Genshaft, private communication).

Such properties of the N boundary as stable depth, alterating high and low velocities, change of reological properties suggest that it is a physical boundary which might represent not only a transition from solid state to liquid state through creep, film and/or partial melting, but also changes in fluid content, transition into the state of true plasticity and other physical transformations. The physical boundaries can produce an irregular distribution of fluids with depth and an increase or a decrease in fluid content at some depth level can provoke the beginning of physical-chemical transformation of matter, new degrees of its metamorphism, and stimulates partial melting at relatively low temperature. The latter processes were found to have operated in old pyroxenites and websterites in the low velocity zones in the lithosphere of the Siberian Craton from geochemical data (Solov'eva et.al.,1989). Higher concentration of the fluids in the cold lithosphere at the depth of 100 km is also suggested by electro-magnetic studies in the Baltic shield (Kovtun and Porokhava, 1980) which observed a high conductivity zone at this depth.

A cause of the irregular distribution of fluids in the upper mantle might also be transition of the ultra-basic rocks in the state of true plasticity (Nikolaevsky, 1985). This means not only change of the rock reological properties but a change in the fluid regime as well. The true plasticity state produce a layer impermeable for fluids which would concentrate beneath or below this layer. Such zones may occur in the

bottom of crust due transition of the asid rocks in the true plasticity state and at depth around 100 km in the mantle due to the same transition of ultra-basic rocks (V.N.Nikolaevsky, private communication). The transition level depends not only on physical properties of the material and pressure but on the temperature as well. The latter may explain why the N boundary depth is shallow in the high heat flow area (80-90 km) and deeper in the cold platform areas (100-110 km).

The processes mentioned above can produce near horizontal ductile zones with inner thin layering. Flow of the mantle matter along these zones might be a cause of preferred orientation of the olivine and formation of the anisotropic high velocity boundaries. The N boundary may be one of these boundaries. It means that the ancient weak zones of the mantle rocks transformation with signs of partial melting might be presented now by high velocity layers, and the velocity inversions observed beneath these layers may be considered as a normal isotropic mantle. Such interpretation is opposite to usual referring the low seismic velocities to the weak (asthenospheric) layers. At any case all processes described can result in the creation of a wide mobile zone which may be considered as the bottom of the mechanical lithosphere.

The data presented highlights the ambiguities that can arise when attempting to define the lithosphere-asthenosphere system. They have shown that plastic or mobile layers may appear within the "thermal lithosphere" and that the asthenosphere is also stratified. The "mechanical lithosphere" is underlain by a weak layer at a depth of around 80-100 km (Fig.17). The "thermal asthenosphere", outlining a set of partly melted zones, coincides with this layer in the areas of active tectonics and uplifts over it in the anomalous high heat flow regions. Beneath old platforms the thermal asthenosphere is located deeper. It would be also noted, that the net of weak zones and layers may be the major channels for mantle material transportation (Fig.15). This suggests that during tectonic processes the flow of mantle matter through these channels may play a more important role than classical convection. Such flow may be considered as a likely mechanism of the advection as well.

II THE UPPERMOST MANTLE LATERAL INHOMOGENEITY OF THE SIBERIAN CRATON.

As shown in the section I, on many seismic profiles anomalously high velocities were observed in the uppermost mantle of the Siberian Craton. Sometimes they reach 8.5-8.6 km/sec at a very shallow depth - directly at the M-boundary. The highest values (up to 8.9 km/s) were observed at this boundary from the traditional deep seismic sounding with chemical explosions as well. They were associated with the kimberlite fields in Western Yakutia (Uarov, 1981, Suvorov at.al., 1985). Such velocities are very difficult to interpret in terms of mantle composition because no rocks are known with such properties (Christensen, 1984, Kern, 1993, Sobolev @ Fuchs, 1993). In papers (Fuchs, 1979, 1983) seismic anisotropy was considered as a more realistic cause of the high mantle velocities. It was difficult to suggest another explanation but there were no enough data to confirm the idea.

The main task of our work was to give new information on the high velocities in the upper mantle in Siberia and to answer the following questions:

- How reliable is the high velocity data, may they be considered as real ones?
- What are characteristic features of the high velocity areas: dimension, depth of penetration and formation?
- Are there some regularities in these areas of high velocity, do they correlate with tectonics and other geophysical fields?
- What are the possible cause of the anomalously high velocities, and, especially, is there an evidence for velocity anisotropy.

In order to answer the questions, the GEON long-range profile data were analysed with main attention on the uppermost mantle waves recorded as first arrivals at distances of 200-1500 km (their maximum depth of penetration is around 200 km).

a. The observed wave fields.

The most reliable data were obtained on four geotraverses which have the best systems of observations with several reversed and overlapping profiles. They are (Fig.1): "Rift", "Meteorite", "Craton" and "Kimberlite" profiles crossing the Siberian Craton in different directions. The most detail analysis of the wave pattern with determination of 2-D models for the crust and upper mantle were made for the "Rift" and "Meteorite" profiles.

Figures 2, 3, 5, 6,18-20 show the record sections, travel-time curves, amplitude plots and of mantle waves and the 2-D models obtained for these profiles.

The travel time patterns of the waves change from one profile to another and along each profile as well. The most stable and simplest picture is observed along the "Craton" (Fig.24). The travel times of the first arrivals form a compact group with continuous increasing apparent velocities from 8.2 km/s at distances 200-300 km to 8.7 km/s at 1800-2000 km. The average travel time curve for this profile will be considered as the 'normal' one.

The wave pattern for the other profiles is more complicated. A typical difference between the observed and the 'normal' travel times due higher velocities of the Pn waves. An extremely wide velocity range of 7.8-8.6 km/s is characteristic for the Pn wave and anomalously high (higher than 8.4 km/s) velocities are often observed. In some cases the high velocities of the Pn waves make it impossible to separate them from the P_N waves (SP M1, R1, R3, K2 and others), but the different attenuations are always characteristic of the Pn waves. Very often the high velocity Pn waves are separated from the P_N arrivals by shadow zones and time delays (Fig.5,19, SP R2, K4, M2).

The strong horizontal inhomogeneity of the upper mantle is also followed from differences of the observed wave fields from the reversed shots on the same profile. An example might be the "Rift" profile.The three principal wave groups described above are clearly observed here from two overlapped shot-points R1 and R2 (Fig.18,19). But their characteristics (apparent velocities and arrival times) are different. From the reversed shot R3 (Fig.20) the wave pattern is impossible to divide in any separate waves. This shot was not recorded by the seismic stations at the distances from 100 to 700 km, so the Pn wave features are not known here. It is difficult to pick up the first arrivals and regular phases in the secondary arrivals as well. The first events are very weak and after them an intensive group of waves with the same velocities around 8.4 km/s was recorded. A strong change of the wave pattern is observed in the middle part of the craton (1300 km of the "Rift" profile, Fig.22): the times from both shots R1 and R2 increase and the high apparent velocities (up to 8.7 km/sec) are characteristic here for both P_N and P_L waves. From reversed shot such velocities does not observed. The same differences between the wave fields from the reversed shots were observed on the "Meteorite" profiles (Fig.23).

b. The uppermost mantle structure.

For all profiles the velocity models were constructed by the ray-tracing method using the data from PNE's and the chemical explosions as well. They show many similar features in the vertical and horizontal inhomogeneity of the upper mantle for the parallel profiles. The profiles "Craton" and "Kimberlite" cross the Siberian Craton from west to east and show also the upper mantle structure of the West Siberian young platform. In both profiles the craton is characterized by higher velocities in the upper mantle if compared with the West Siberian platform. And anomalous high velocities are observed in the western part of the "Kimberlite" profile.

The "Rift" and "Meteorite" profiles cross the Siberian Craton in N-S direction and characterise the mantle structure of two rift zones: theBaikal Rift and theYenisei-Chatanga Rift with the Pur-Gedan Basin. The relatively low velocities (7.9-8.0 km/s) are observed in the high heat flow regions: the Baikal Rift and the Pur-Gedan basin. The low velocity block is also observed in the central part of the craton near the Low Angara basin.

Unusual features of the craton upper mantle structure are the inversion zone at the depth of 100 km which located in the lithosphere. In "Rift" profile it was determined as the most reliable but only in the south part of the craton. The strong reflected boundary underlines this zone, it dips to the central part of the craton. The boundary was constructed from the waves P_N. The velocities beneath the boundary are 8.5-8.6 km/s. For the inversion zone it is impossible to determine a unique velocity model, its thickness depends on the average velocity in the zone. We suggested the velocity of 7.9 km/s as the most probable velocity at this depth interval and got the thickness of the inversion zone 20 km. For comparison, if the velocity of 8.1 km/s were taken it increase the zone thickness up to 30 km. The inversion zone flatten out in the middle part of the craton where the crustal structure is changed too. It looks not occasional and shows a correlation between geological history and the upper mantle structure.

The most impressive feature of the craton inhomogeneity are however the high velocity blocks. Two blocks (500 km long) of anomalous high velocities (8.4-8.6 km/s) are determined: in the central part of the Tunguss depression (Tunguss block) and in the south part of the craton near to the boundary with the Baikal Rift (Pre-Baikal block).

In the Tunguss block (interval of 800-1500 km in "Rift" profile) the reversed travel-time curves show first arrival apparent velocities of 8.4 km/s. The Pn wave from SP R2 and the chemical SP173,192,185 has these high velocities at minimal distances from the shot, which means that directly beneath the M-boundary velocities of around 8.4 km/s are observed. On the "Meteorite" (Fig.23) the Tunguss block is characterised by two reversed travel-time branches with velocities 8.4 km/s, over the 1500-1700 km interval of the profile.

The Tunguss block was crossed by "Kimberlite" profile in the interval 1000-1200 km where the Pn wave from SP K2 has a velocity of 8.7 km/s and overlapping travel time curves also show a relative increase in apparent velocities up to 8.8 km/s. Continuation of the block to the east might also be suggested from the high velocities of the first arrivals of SP K1 and K2 at 1400-1600 km, but it is not clear if these velocities are not due to deeper parts of the mantle.

The high velocities in the Pre-Baikal block follow from the times of the first arrivals of SP R3 and the chamical SP 72, 78, 67, 58, on the "Rift" profile where the Pn velocities are 8.5-8.6 km/s in both directions (Fig.22, 2000-2500 km interval of the profile). The "Meteorite" profile in the area of this block has two reversed Pn branches with a velocity 8.6 km/s over the interval 2100-2300 km (SP M3, M4).

The boundary between the high and low velocity blocks are near vertical or inclined like the northern boundary of the Pre-Baikal block subducted beneath the central part of the Siberian Craton. Such a structure is deduced from the both profiles. The real form and the exact dipping angle of the subducted boundary is difficult to determine because no clear waves reflected from the boundary were recorded. The boundary was introduced into the cross-section using ray tracing modelling to explain the observed peculiarities of the travel times curves at 1800-2200 km on the "Meteorite" and at the 1400-1800 km on the "Rift" profiles. In both cases a local decrease in the times from the northern shots (M1, M2, R1, R2) were recorded in these intervals of the profiles, on the reversed branches (SP R3 and M4) there are no sharp changes in the travel times. The inclined boundary between low and high velocity blocks subducted beneath the central part of the craton can explain these wave peculiarities.

In all high velocity cases mentioned the record intervals (length of the travel time curve) is 200-500 km. Crustal structure usually does not change strongly in these intervals to effect the Pn velocities. The

records are clear and the first arrival correlation is not difficult. Thus, there can be no doubt that such high velocities are realistic.

c. Nature of the high velocity blocks, velocity anisotropy.

The nature of the observed velocity inhomogeneity of the craton upper mantle is not easy to explain, especially the anomalous high velocities. This problem has been discussed in many papers (Fuchs, 1979, Egorkin and Pavlenkova, 1981, Sobolev & Fuchs,1993) but still remains obscure. That is why any new information on the problem, for instance, on correlation of the mantle velocities with other geophysical fields and tectonic features or on the velocity anisotropy is very important.

Upper mantle horizontal inhomogeneity are usually correlated well with the geological history of the region or with the temperature regimes: i.e. low velocities are observed in the high heat flow rift regions: the Baikal Rift, the West Siberian rifts. The young West Siberian platform is also different from the old one with a relatively lower mantle velocities.

But regarding the correlation between the anomalous high velocity blocks and the geophysical fields or the tectonic features of the Siberian Craton, it is difficult to make definite conclusion. The heat flow is very low in all regions of the craton (Kutas @ Smirnov, 1991) and it does not correlate with the mantle velocities. The magnetic field in general is different in the western part of the craton where the high velocity blocks are located. This part is an area of the Tunguss depression with large amount of the plateau-basalts. The latter are the cause of the complicated short-wave length magnetic field anomaly. However, the high velocity blocks have no direct correlation with observed plateau-basalt intrusions or with the local magnetic anomaly pattern.

A detailed analysis was made to investigate how the high velocity blocks are reflected in the gravity field. Two methods of analysis were used . The first, involved the calculation of the crustal gravity effect using laboratory data on the relationship between P- and S-velocities and densities and then subtracting this effect from the observed Bouguer gravity anomalies. The differences between these two fields may be considered as mantle anomalies. In this study no positive anomalies were found in the areas of high mantle velocities. The second method involved a gravity inversion using density models and determining relationships between velocity (v) and density (d) in the different layers of the crust and upper mantle. These relationship are presented in Fig.26. They show clear v-d correlation in the crust (velocities from 6 to 7,5 km/s) and no correlation in the mantle velocityinterval (more than 7.5 km/s). This result means that the high velocity blocks have no higher densities.

Thus, no evidence exists to explain anomalous high velocities in the uppermost mantle of the Siberian Craton with change of composition or temperature regime. The only possibility is seismic anisotropy. There is now little doubt that the upper mantle is anisotropic and there is a considerable amount of seismic evidence for the presence of anisotropy beneath the continents (Bamford, 1977, Fuchs, 1979, 1983, Babushka et.al.,1984). However, in many cases the currently available data do not discriminate between seismic velocity anisotropy and horizontal inhomogeneity. Without a special observation the velocity anisotropy may be artefact which are due to the biased sampling of laterally varying refractor velocities. Such a situation exists in Siberia.

There has been no special investigation of velocity anisotropy here. Unsure situation occurs with the long-range profiles as well. They cross each other, but this is not enough to discriminate the vertical and horizontal inhomogeneity from other effects. The first impression created was that there is no difference in the velocities between the crossing profiles, and some of them ("Kimberlite" and "Meteorite") show the anomalous high velocities in both directions (Fig.23,25). So it looked like an azimuthal anisotropy was not the cause of the anomalous high velocities. This however, does not mean that the azimuthal anisotropy does not exist at al. Sometimes regular differences in the Pn -velocities and arrival times of the P_N waves are observed, when crossing profiles are compared. In the N-S direction

the mantle velocities are a little bit higher than in the W-E direction. Some differences are observed in the amplitude curves as well: in average along the W-E profiles the Pn attenuation is on average stronger than along the N-S profiles (Fig.21b).

But such a suggestion is very uncertain for Siberia. The differences in travel times of the crossing profiles might be a result of the complicated structure of the mantle rather than anisotropy. An unambiguous comparison of the Pn velocities at different azimuths was found impossible. As seen from Fig.27b, only at one cross-point ("Rift and "Craton" profiles) does the Pn wave cover the common depth interval (SP C2, R1 and R2). But differences in the Pn velocities are not clear because of the complicated form of the observed travel time curves caused by the crustal structure. For the other crossing points there are no common depth coverage. Comparing the nearest shots for the "Kimberlite", "Rift" and "Meteorite" profiles no differences between Pn velocities are observed, in both directions they are very high.

So the present observation scheme does not permit the unambiguously determination of azimuthal anisotropy in the upper mantle of Siberia but another kind of the anisotropy wherein the velocity is higher in the near horizontal direction than in the vertical one can explain the observed data..

. Thus the main results of the studies of the upper mantle lateral inhomogeneity in Siberia are the following:

1. In general the horizontal inhomogeneity of the upper layer correlates with the crustal and tectonic age and with heat flow. Relative low velocities are characteristic for the young West-Siberian platform and for the Baikal Rift. But the old Siberian Craton is the exception to this rule.

2. Inside the Siberian Craton the seismic velocities beneath the Moho vary from 8.0 to 8.6 km/s. Usually the velocity variations are observed in narrow zones between large mantle blocks. The block structure penetrates down to depths of 100-110 km. Two blocks with anomalously high velocities (8.5-8.6 km/s) were outlined in the western part of the craton. The observed gravity, magnetic and heat flow fields do not correlate with the high velocity blocks.

3. Assuming that normal uppermost mantle velocities can not be higher then 8.3-8.4 km/s the observed anomalous high values may be considered as an effect of velocity anisotropy but not an azimuthal one because the high velocities are observed in different directions.

III. METHODS OF DYNAMIC IMAGING OF THE DEEP SEISMIC SOUNDING DATA. AND COMPARISON OF THE P- AND S - WAVE PATTERN.

a. Migration of the crustal wide-angle reflections

At deep seismic sounding (DSS) by wide-angle reflection and refraction method only some regular waves traced for distance more than 20-50 km are used for the interpretation. The travel times of these waves are usually interpreted in form of 1-D or 2-D velocity models. The latter are show structure of some sharp boundaries and of velocity isolines. Synthetic seismograms calculated for such models are considered well fitted to the observed ones if they show correct times of the waves, used for interpretation and if the wave amplitudes relation are comparable with observed ones. But these waves are usually a small part of the whole observed wave pattern. Besides, the basic wave are usually complicated wave groups and only the first arrival of these groups are used for the model construction. Other information on the wave group pattern are left for the interpretation. Future development of the wide-angle reflection method no doupt depends on increasing information taken from the records: all wave pattern, the basic wave peculiarities, their coda and all random phases, considered now as a 'seismic noise' should be used for the seismic imaging of the lithosphere. One of the ways of such interpretation might be migration of wide-angle reflections and refractions. Methods the near-vertical reflection

migration at CDP have shown how perspective may be such proceeding of the seismic records for imaging heterogeneous media like the crust.

The wide-angle reflection migration is much more complicate problem than the near-vertical reflection migration due to low dense of the observation at the DSS profiling. The principal of the migrations are the same. The subsurface is divided into an equally spaced grid in which grid points are treated as secondary source points. All reflected or diffracted energy are calculated in each grid points. The migrated section is than constructed by summing along diffraction curves the contributing of the observed wave field. Superposition principle is working, such that contributing amplitudes along diffraction curves reinforce at the correct subsurface points and destructively interfere at all other locations. The later means that a lack of coherency in the direction predicted for the model results in amplitude suppression. To get good results high-fold wave field data like at CDP are necessary.

We made an attempt to apply the migration technique to ridely spaced and low-fold wave field data as the ordinary wide-angle reflection data. The general questions were discussed if the processing techniques, like a migration, can be used for such data and what migration algorithm can give a stable solution for source-receiver distances much larger then the depth to reflector.

The migration method, developed by V.N.Pilipenko (1982) for the refraction and wide-angle reflection data was applied. The method based on finite-difference solutions of the time and wave equations on the special grids. Two solutions are obtained independently: the time fields are calculated on 2-D space (depth-distance) grid, the wave fields - on 3-D space-time grid. The time fields are continued from the point source to the grid points; the reflection wave fields are continued from the surface, where they were recorded into the medium and determined at a set of depth levels. Specific feature of the method used is a special transformation of the grids for different types of waves. It is important because for very large scale problems such as imaging features (tens of kilometres deep) from wide-angle data (with source to receiver distances from zero to beyond 200km), finite-difference extrapolations became impractical, as the ordinary grids involved are excessively large. In Pilipenko's algorithm the grid lines are curved and follow the rays and wave fronts. This increases accuracy of the wave field continuation and excludes the points where the wave equation solution can not be obtained. The study have shown that a stable time field determination for large distances from the source and for inhomogenious media is possible if the finite-difference solution of the eiconal equation is found on the orthogonal grid formed from the seismic rays and isochrones at linear change of seismic velocities. The velocity gradients for the grid parameter valuation are determined from the velocity model averaging.

The method may be applied to other types of waves, for instance, for the refractions. In this case two reversed wave fields (the groups of the first arrivals) are continued from the surface into the medium and determined at a depth level where the sum of travel time are equal to the reciprocal time. At a dense system of the observations, which usually used in Russian seismic prospecting for tracing the basement surface this migration method gave excellent result. One of example is shown in Fig.28 for complicate structure of the basement in Dnieper-Donets Basin.

The DDS's have no dense enough observations and we have chosen one of the best profiles from this point of view, the "Polar" profile in Northern Scandinavia (Luosto et.al.,1989). On this profile the data were collected using 3-component seismic stations spaced in 2-3 km along profile. The seismic energy from 9 shots (A, B, C, R, T, D, S, E, F), located along the profile with intervals of 20-80 km was recorded at distances from 0 up to 200-300 km. (Fig.29). Good quality records were obtained for all shot-points .

The observed fields on the "Polar" profile may be considered as a typical for the wide-angle reflection survey in the Baltic Shield (Fig.30 and 31 show P- and S records for the shots A and F). The most intensive reflections both in P- and S-wave fields were traced from the Moho and several crustal

reflections were recorded as well. The Moho reflection pattern is complex and changes along the profile. The records show also different features of the crustal waves for different tectonic blocks.

The differences may be illustrated by Fig.30 and 31. In the south part of the profile (Karasjok- Kittila greenstone belt, Proterozoic block, SP A) the first arrival of Pg and Sg waves are surely traced up to distances of 100 km from the source, then clear shadow zones observed up to distance of 150 km. The Moho waves are of high amplitudes from the shot A. In the northern part of the profile the wave fields from SP F (Sorvaranger Terrain, Archean block) have no such clear shadow zones (especially for P-waves) and have no distinct arrivals of the Moho reflections. There are also differences in P and S wave fields from the same shot. The Sn waves in all cases are of lower amplitudes in comparison with Pn waves. The crustal arrivals (K2 wave in Fig.30) are well correlated in the P- wave records from SP A and they are very poor in the S- wave fields. It was very important to know how these differences are distributed in space along the profile and how they correlate with tectonic structure. The migration technique helped us to show this in form of depth-migrated cross-sections (Fig.32).

To get these images we have used a single-shot gather of 175-200 traces extending from 25 to 200-225 km with a reduced time window of 0 to 12 sec. The 2-D velocity distribution given in (Luosto et.al.,1989) was used for the migration. As soon as the velocity model determination is not unique, especially for the lower crust, before the record proceeding a number of migration velocities were tested. The tests showed that the velocity changes in 0.1-0.2 km/sec influenced on the depth of the reflectors but not on the result of the constructive or destructive interference of the wave fields. The latter is stable enough and it allowed to use a simplified velocity model for the migration.

The depth-migrated images of the crustal structure obtained for both P- and S wave fields looks realistic (Fig.32). They contain large-scale elliptical noise patterns with source and receiver as foci (migration smiles) in the upper part of the cross-section where there are not enough observed data to suppress this coherent noise. There are also some noise background formed by the migration ‘smiles’ in the lower part but some specific features of the lower crust and of the Moho structure clearly observed (lines in the Fig.32 show velocity isolines, obtained from the travel-time interpretation by ray tracing method). In the southern part of the profile (Karasjok- Kittila greenstone belt, Proterozoic block) the Moho is traced as a sharp boundary at a depth of 45 km. Beneath the Lapland Granulite Belt it uplifts up to 40 km and there are places where the boundary correlation is interrupted (probably they correspond to deep fault zones). In the northern part of the profile (Sorvaranger Terrain, Archean block) the Moho looks like heterogeneous layer, but it is possible to trace the boundary as a top of the layer and to show that the thickness of the crust does not increase to the north as it was shown in previous interpretation.

An impressive feature of the cross-sections is the boundary K2 at a depth of 35 km in the Proterozoic block which is well traced in the P-wave field and does not exist in the S-wave field. It means that there is a principal changes of the rock composition in the lower crust of this block. This change produces the change of the Vp/Vs ratio at the boundary K_2.

There are not enough data to get good images for the upper crust, however some of dipping boundaries traced from geological data beneath the shots C-D probably are reflected in the migration cross-section.

The migration images were compared with the mid-point transformations (an NMO - corrected CDP gather) made for the same wave fields (Fig.33). The transformations contain the observed wave fields without migration artefacts and in general they look similar to the migration field, but some characteristic features of the low crust look not so clear in the case.

b. Comparison of the migration data with P- and S- velocity models.

A comparative analysis of the crustal P- and S- velocities were made to get more information for the geological interpretation of the depth migration cross-section. The first interpretation of the 'Polar' data (Luosto et.al.,1989) showed no change of the P- and S-velocity ratio (Vp/Vs) in the middle and lower crusts. The comparison of the observed travel-times of the P- and S-waves showed however that the difference exists. In Fig.30 the travel-time curves of the Pg- and Sg- waves are the same for SP A up to distances of 80 km. It means that in the upper crust the Vp/Vs ratio is 1.73 (this value corresponds the reduction velocities of 8.0 km/s for the P wave record-section and of 4.62 km/s for the S- waves). At distances of 100-200 km the first arrivals of Pg (wave K2) are of high amplitudes but it is impossible to trace this wave in the S-records (there are some low amplitude phases at the higher arrival times which might be interpreted as increasing of Vp/Vs ratio in the middle crust, but they are very uncertain). Clear difference in the arrival times are observed for the Moho reflection: the PmP times are much lower than SmS times. The latter suggests increasing of Vp/Vs ratio in the lower crust up to 1.8.

For SP F another relation between Pg and Sg travel times is observed. The Pg has lower velocity than Sg and Vp/Vs ratio decreased here down to 1.7. This value corresponds to the upper and middle crust where the Pg and Sg waves penetrated. As regards the lower crust in this part of the profile it is difficult to say some things definite because of very poor waves from the Moho.

The determined values of the Vp/Vs velocity ratio are shown in Fig.29. They explain why the K2 boundary is clear traced in the P-wave migration cross-section and does not exist in the S wave image. At this boundary P- velocity increases but the S-velocity remains the same. Correspondingly the Vp/Vs value increases. The observed relation suggests the boundary between falsic and basic rocks and existence the basic rocks in the lower crust of Karasjok- Kittila greenstone belt, Proterozoic block. In contrary the crust of Sorvaranger Terrain, Archean block is composed mainly from felsic rock. It should be noted that this result became possible only due to the combine interpretation of P- and S- wave fields. The only P-wave data show similar velocities in both blocks. The Vp/Vs ration allowed to discriminate these tectonic elements and show that the Archean crust is more felsic than the Proterozoic one. The observed Vp, Vs and Vp/Vs values have also shown that the high velocities (6.8-7.0km/s) in the lower crust are due mafic composition in the young block and to a higher degree of metamorphism of felsic rooks in the older block.

The main conclusion of the studies made is that the dynamic images of the crust obtained with wave field migration allow to get more information from the records and the methods of the migration are very perspective for future development. But to use advances of the methods it is necessary to made more dense
observations at the wide-angle reflection survey.

List of papers prepared for publications as the results of the project work

1. Pavlenkova N.I. On a global seismic boundary in the upper mantle, Physics of the Earth, N 12, 1995, 1-12.
2. Egorkin A.V., Pavlenkova N.I., Romanyuk T.V. Solodilov L.N. Upper mantle structure along the Rift profile. Accepted for publication in Geology and Geophysics
3. Pavlenkova N.I. General features of the uppermost mantle stratification from long-range seismic profiles. Accepted for publication in Tectonophysics.
4. Pavlenkova N.I., Pavlenkova G.A., Solodilov L.N. High velocities in the uppermost mantle of the Siberian craton.Accepted for publication in Tectonophysics.
5. Pavlenkova G.A., Solodilov L.N. Anomalous high velocities in the upper mantle of Siberia. Accepted for publication in Physics of the Earth.

References

Andersen, D.L., 1989. Theory of the Earth. Blackwell scientific publication, Boston, 366 pp.

Ansorge, J.,Bonjer, K.P. and Emter, D., 1979. Structure of the uppermost mantle from long-range seismic observations in southern Germany and the Rhinegraben area, Tectonophysics, 56, 31-48.

Babuska, V., Plomerova, J. and Sileny, J., 1984. Spatial variations of P residuals and deep structure of the Europian lithosphere. Geophys. J.R. Astron. Sos., 79: 363-383.

Bamford, D., 1977. P -velocity anisotropy in a continental upper mantle. Geophys.J.R.A.S., 49, 29-48.

Benz, H.M., Huger, J.D., Leith, W.S., Mooney, W.D., Solodilov, L.N., Egorkin, A.V. & Ryaboy, V.S.,1992. Deep seismic sounding in Northern Eurasia. EoS, 73, 297-300.

Benz, H.M., McCarthy, J., 1994. Evidence for an upper mantle low velocity zone beneath the southern Basin and Range-Colorado Platean transition zone. Geophys. Res. Lett., vol 21, 7, 509-512.

Boyd, F.R. 1984. Siberian geotherm based on lherzolite xenoliths from the Udachnay kimberlite, USSR. Geology, v.12, N 9, 528-530.

Christensen, N.I., 1984. The magnitude, symmetry and origin of upper mantle anisotropy based on fabric analyses of ultramafic tectonites. Geophys. J.R. Astron. Soc., 76: 89-111.

Cipar, J.J., Priestley, K., Egorkin, A. & Pavlenkova, N., 1993. From rift to rift: the Yamal Peninsula - Lake Baikal deep seismic sounding profile. Geophys.Res.Lett., 20, 1631-1634.

Egger, A., Demartin, M., Ansorge, J., Banda, E. & Maistrallo, M., 1988. The gross structure of the crust under Corsica and Sardinia, Tectonophysics, 150, 1988, 363-389.

Egorkin, A.V. and Kun,V.V., 1978. P-wave absorption in the upper mantle of the Earth. Physics of the Earth, 4, 25-36

Egorkin, A.V. & Chernyshov, N.M., 1983. Peculiarities of mantle waves from long-range profiles. J.Geophys., 54: 30-34.

Egorkin, A.V., Zuganov, S.K., Pavlenkova, N.A. & Chernyshev, N.M., 1987. Results of lithosphere studies from long-range profiles in Siberia.Tectonophysics, 140., p.29-47.

England, P., Kennet, B., Worthington, M.,1978. A comparasion of the uppermantle structure beneath Eurasia and the North Atlantic and Arctic Oceans - Geoph.J.R., astr.Soc., 54, 575-585.

Fuchs, K.,1979. Structure, physical roperties and lateral heterogeneities of the subcrustal lithosphere from long-range deep seismic sounding observation on continents. Tectonophysics, v.56, 1-15.

Fuchs, K., 1983. Recently formed elastic anisotropy and petrological model for the continental subcrustal lithosphere in southern Germany. Phys.Earth Planet.Inter., 31, 93-118.

Fuchs, K. @ Froidevaux, C. (Eds.),1987. Composition, structure and dynamics of the lithosphere-asthenosphere system. M.Geophys.Union, Geodyn.Ser., 16.

Gordienko,V.V. and Pavlenkova, N.I., 1985. Combined geothermal-geophysical models of the Earth's crust and upper mantle for the European continent. J.Geodynamics, 5: 75-90.

Grad, M., 1987. Seismic model of the Earth's crust and upper mantle of the east European platform. vol XXXV, N2, 121-155.

Guggisberg, B., Kaminski, W. & Prodehl, C., 1991. Crustal structure of the Fennoscandian Shield, a traveltime interpretation of the long-range FENNOLORA seismic refraction profile. Tectonophysics, v.195, N 2/4, 105-138.

Hales, A.L.,1969. A seismic discontinuity in the lithosphere, Earth and Planet.Sci.Lett., 7, 44-46

Hales, A.L., K.J.Muirhead, J.M.Ryan and J.F.Gettrust, 1975.Upper mantle travel times in Australia - A preliminary report, Phys Earth Planet.Inter.,11, 109-118

Hirn, A., Steinmetz, L., Kind, R., @ Fuchs, K., 1973. Long range profiles in Western Europe: Fine structure of the lower lithosphere in France (Southern Bretagne). Z.Geophys., 39, 363-384.

Hirn, A., Steinmetz, L. & Sapin, M., 1977. A long range seismic profile in the Western Mediterranean Basin: structure of the upper mantle. Ann.Geophys., 33: 373-384.

Jordan, T.H., 1981. Earth structure from seismological observations, Physics of the Earth's Interior, A.M.Dziewonski, E.Boschi (Eds.), North-Holland, Amsterdam, 1040.

Kern,H., 1993. P and S-wave anisotropy and shear wave spliting at pressure and temperature possible mantle rocks and their relations to the rock fabric. Phys. Earth Planet. Inter., 78: 245-256.

Kovtun,A.A. & Porokhava,L.N., 1980. Deep conductivity distribution on the Russian platform from the results of combined magnetotelluric and global magnetovariational data interpretation. J.Geomag.Geoelectr., v.32, suppl. 1, 105-133.

Kutas, R.I. & Smirnov, Ya.B., 1991. General evolution of crustal structure of the USSR territory. In: Beloussov,V.V., Pavlenkova,N.I. and Kvjatkovskaya,G.N.(Eds.), Deep Structure of the USSR Territory. Nauka, Moscow, pp.186-192.

Lie,J.E., Pedersen, T. and Husebye, E.S., 1990. Observations of seismic reflectors in the lower lithosphere beneath the Suagerran, Nature, 6280, vol.346, 165-168.

Luosto, U., Fluch, E.R., Lund, C.E., and working Group, 1989. The crustal structure along the Polar profile from seismic refraction investigation. Tectonophisics, 162, 51-55.

Matveeva, N.N. and Pavlenkova, N.I., 1983. Results of 2-D and 3-D numerical modeling of the crust beneath the Iceland. In: Physics of seismic waves andinner structure of the Earth. Moscow, Nauka, 171-179 (In Russ.).

Mechie, J., Egorkin, A., Fuchs, K., Riberg, T., Solodilov, L. & Wenzel, F. P-wave mantle velocity structure beneath Northern Eurasia from long-range recordings along the profile Quartz, Phys. Earth Planet. Inter., 79, 269-286.

Morelli, C., Cassinis, R., Giese, P. and Rower, P.,1977. Structure of the lithosphere of the Italian Peninsula, Publ. Inst. Geophis. Pol.Acad.Sc., A-4 (115), 451-456

Morquart, G. & Lelgemann, D. 1992. On the interpretation of geoid anomalies in Europe with special regard to the EGT profiles, Tectonophysics, v.207, N 1/2, 25-42.

Mueller, St. and Ansorge, J.,1988. Deep seismic sounding of the mantle lithosphere, In: G.Nolet and B.Dost (Eds.), European Geotraverse (EGT) Project, the upper mantle. ESF, Strasbourg, 63-76

Nikolaevsky, V.N., 1985. Mechanics of fluid-saturated geomaterials: discusser's report. In: Z.Bazant (Ed.), Mechanics of Geomaterials. Wiley, NY, pp. 379-401.

Pansa, G.F., Mueller, St. and Calcagnile, G., 1980. The gross features of the lithosphere-asthenosphere system in Europe from seismic surface and body waves. Paleophysics, v.118, Birghauses Verlag, Basel, 1209-1213

Pavlenkova, N.I., 1988. The nature of seismic boundaries in the continental lithosphere, Tectonophysics, 154, 211-255.

Pavlenkova, N.I., Pogrebitsky, Yu.E. and Romanjuk,T.V., 1993. Seismic-density model of the crust and upper mantle of the South Athlantic along Angola-Brazil geotraverse, Physics of the Eurth, 10, 27-38.

Pavlenkova, N.I. & Romanyuk, T.V. 1991. Seismo-gravity modeling for the crust of Siberia. Geology and Geophysics, N 1, p.34-42.

Pavlenkova, N.I. & Yegorkin A.V., 1983. Upper mantle heterogeneity in the northern part of Eurasia. Phys. of Earth and Planetary Interiors, 33, p. 180-193.

Pilipenko, V.N., 1982. Continuation of the wave fields by the finite-difference method on the grid. In: Application of the numerical methods in the lithosphere studies. Novosibirsk, Computer Center, 144-154.

Posgay, K., Hegedus, E., Timar, Z., 1988. The identification of mantle reflections below Hangary from deep seismic profiling, In: Seismic probing of continents and their margins, vol 173, Camberra meeting 1990, 379-385.

Priestley, K., Cipar, J., Egorkin, A. and Pavlenkova, N., 1994. Upper-mantle velocity structure beneath the Siberias platform. Geophys. J. Int., 118, 369-378.

Prodehl, C., 1984. Structure of the Earth's crust and upper mantle. In; Landolt-Bornstein, Numerical Data and Functional Relationships in Science and Technology, Group V, vol.2 (Geophysics of the Solid Earth, the Moon and the Planets), Subvol. a, pp 97-206, Springer-Verlag, Berlin.

Research Group for lithospheric structure in Tunisia, 1992. The EGT' 85 seismic experiment in Tunisia: a reconnaissance of the deep structures, Tectonophysics, vol.207, N 1/2, 245-267.

Revenaugh, J and T.H. Jordan, 1991. Mantle layering from ScS reverberation 3. The upper mantle, J.Geophys.Res.,96, 19781-19810

Revenaugh, J. & Sipkin, St.A., 1994. Mantle discontinity structure beneath China. J.G.R., vol 99, B11, 21,911-21,927.

Ryaboy V.Z., 1966. Crust and upper mantle sructure from DSS profile Kapet-Dag - Aral Sea, Sovjet Geology, N 5, 159-162 (In Russ.).

Sobolev,S.V. & K.Fuchs, 1993. Seismic velocities and density in the deep continental lithosphere from the composition of xenoliths. Terra Nova, 5, Abstract suppl.1 EUG V11, Strasbourg, 333-334.

Solov'eva, L.V., Vladimirov, B.M., Kiselev, A.I. and Zavijalov, L.L., 1989. Two stages of mantle metasamatites of deep xenoliths from Yakutia kimberlites and their relation to lithosphere processes. In: Precambrian metasamotites and their ore deposits. Nauka, Moscow, p.3-17./In Russ./

Spakman, W.,1988. The three-dimensional structure of the upper mantle beneath central Europe and the Mediterranean. In: G.Nolet and B.Dost (Eds.) European Geotraverse (EGT) Project, upper mantle. ESF, Strasbourg, 49-57.

Suvorov, V.D., Kreinin A.B. & Podvarkova A.I., 1985. 3-D deep seismic studies in Malobotnobinsk region of Yakutia. Geology and Geophysics, N 1. p. 82-90.

Uarov,V.F., 1981. Seismic peculiarities of the upper mantle of Western Yakutia. Geology and Geophysics,N 9, 120-124

Yegorkin, A.V.and Pavlenkova, N.I., 1981. Studies of mantle structure of USSR territory on long-range seismic profiles. Physics of the Earth and Planetary Interior, 25, pp.12-26

Figure capture

Fig.1 Scheme of the GEON long-range seismic profiles carried out with Peaceful Nuclear Explosions (PNE): R1, R2, R3 in the "Rift" profile, M1, M2, M3, M4 on the "Meteorite", C1, C2, C3, C4 on the "Craton" and K1, K2, K3 on the "Kimberlite", Q1, Q2, Q3 on the "Quartz", H1 and H2 on the "Horizont", Ru on the "Rubin". The tectonic elements: 1 -East-European and Siberian old platforms, 2-Kasach massif, 3 - the Urals.

Fig.2 Record -section from the PNE C1 demonstrates the typical mantle wave pattern and principal wave groups generated in the upper mantle of the Siberian Craton: P_n - apparent velocities of 7.8-8.6 km/s, penetration depth of 50-100 km, P_N - velocity - 8.4- 8.5 km/s, depth - 100-150 km, P_L - velocity - 8.5-8.6 km/s, depth - 150-250 km, P_{410} -a wave from the top of the transition zone between upper and lower mantle at the depth of 410 km , P_{520} - from the boundary at a depth of 520 km and P_{680} - at the top of the lower mantle.

Fig.3. Record -section from the PNE C4. The wave indication are in Fig.2.

Fig.4. Record -section from the PNE Q4 which shows a clear shadow zone at distances 1750-2250 km.. The wave indication are in Fig.2.

Fig.5. Record-section from the PNE M4 which shows anomalous high velocity (around 8.7 km/s) of the Pn waves. The wave indication are in Fig.2.

Fig.6. Record -section from the PNE C2.

Fig.7. Record section from the PNE Ru on the "Rubin" profile characterizing the complicated structure of the N and L boundary waves.

Fig.8. Comparison of the travel-time curves and amplitudes of the uppermost mantle waves at distances from 200 to 2000 km for the PNE's shown in Fig.1. They show a strong difference in the P_n velocities and P_L arrival times but relatively tight arrival times of the P_N waves. Amplitude curves are shown only for the "Kimberlite" profiles but their form typical for the other profiles as well.

Fig.9. Comparison of the travel-time curves of the upper mantle waves at distances from 1600 to 3000 km for the PNE's shown in Fig.1.

Fig.10. Generalized upper mantle model.

Fig.11. Record sections of the uppermost mantle arrivals from the long range profiles in West Europe (a) and sheme of their location (b): FP - Franch profile (Hirn et al.,1973), PB - Provencial Basin (Hirn et al,1977), CS - EGT in Corsica-Sardinia region (Egger et al,1988), SI-long-range profile in South Italy (Morelly et al.,1977), T - EGT in Tunisia. (Res.group., 1992). Intensive secondary arrivals observed after P_n wave: P_1^N, E, P_1 and P_N belong to a boundary at depths of 90-100 km (N - boundary).

Fig.12. a. Travel time curves of the mantle waves for the profiles in West Europe. The waves P_1, P_1^N , E from the records in Fig.11 form the compact group P_N and this was a major reason to refer these waves to the same boundary.

b. The observed travel time curves of the mantle waves for the Brazil Basin along the Angola-Brazil geotraverse (Fig.15).

Fig.13. Comparison of the upper mantle travel times for (1)the North Atlantic, (2) West Europe (England et.al.,1977) and (3) for the Siberia.

Fig.14. Generalized cross-section of the upper mantle for the profile from the North Atlantic to the Siberian Craton.

Fig.15. Scheme of the DSS profiles and a preliminary cross-section along the Angola-Brazil Geotraverse: 1 - observed Bouger anomalies, 2 - observed Fai anomalies, 3-5 - calculated model gravity effects for the crust (3) and for the upper mantle (4,5) with different relations between seismic velocities and densities (Pavlenkova et al., 1993), 6 - heat flow, 7 - magnetic field.

Fig.16. Record section of the mantle waves for the Brazil slope of the mid-oceanic ridge in the Angola-Brazil Geotraverse (profile V in Fig.8): P_n - the Moho refraction, N_1 and N_2 - reflections and refractions from the mantle boundaries shown in Fig.8.

Fig.17. General rheological model of the crust and upper mantle structure for the continent. 1 - brittle upper crustal layer with strong horizontal inhomogeneity and with many faults flattening out at the layer bottom, 2 - weak (ductile) layer in the middle and lower crust, 3 - high velocity and brittle lower crust which is typical for old platforms and central parts of continents, 4 - uppermost mantle layer with normal velocity (8.0-8.2 km/s), 5 - with higher and, 6 - with lower velocities, 7 - rheologically weak layer of upper mantle, 8 - partly melting zones - asthenolites, 9 - bottom of the 'thermal lithosphere, 10 - the N boundary discussed in the paper, which devides upper mantle layers with different rheologies and is considered as a bottom of the ‘mechanical lithosphere’.

Fig.18. Record-section from the PNE R1 on the "Rift" profile.

Fig.19. Record-section from the PNE R2 to the south on the "Rift" profile which show a clear shadow zone with the strong time delay between the P_n and P_N waves indicating a velocity inversion in the Siberian lithosphere.

Fig.20. Record -section of the upper mantle waves from the SP R3 on the Rift profile.

Fig.21. Comparison of the travel-time curves (a) and amplitude curves (b) of the uppermost mantle waves (the first arrivals at distances from 200 to 2500 km) for PNE's of the profile "Rift'.

Fig.22. The observed travel-times of the mantle waves and the 2-D model of the upper mantle for the "Rift" profile.

Fig.23. Seismic cross section and the observed travel-time curves for the profile "Meteorite"

Fig.24. The observed travel-time curves and seismic cross-section for the profile "Craton" (Egorkin at.al., 1987).

Fig.25. The observed travel-time curve and seismic cross-section for the profile "Kimberlite" (Egorkin at.al., 1987).

Fig.26. Experimental relations detween seismic velocities and densities determined as a result of the gravity modeling for the Siberian long-range profiles.

Fig.27. Comparison of the travel-time curves of the uppermost mantle waves (the first arrivals at distances from 200 to 2500 km) for the crossed profiles "Rift", "Meteorite", ~~"Craton"~~ and "Kimberlite" (a) and a scheme of the Pn wave caverage of the subcrustal lithosphere (b). Only in one crossing point (SP R1, R2, C2) the waves have a common depth interval of penetrating.

Fig.28. Results of the migration imaging the basement surface from the refraction data in the Dnieper-Donets basin. The refraction boundary is shown on the background of the sedimentary structure obtained from the CDP data.

Fig.29. The crustal velocity cross-section for the "Polar" profile (Luosto et.al., 1989). The velocity values in brakes were determined by the authers.

Fig.30. Record-section of the crustal waves from SP A on the "Polar" profile. The reduction velocity is 8.0 km/s for the P record-section and 4.62 for the S records. It corresponds to Vp/Vs ratio of 1.73. The dotted lines show the travel-time curves of the P-wave arrivals.

Fig.31. Record-section of the crustal waves from SP F on the "Polar" profile

Fig.32. Depth migrated cross-sections. obtaned from the P-wave fields (a) and from the S-wave fields (b), the "Polar" profile. The dotted lines show location of the Moho boundary from Fig.29.

Fig.33. Mid-point transformations of the P-wave fields (a) and the S-wave fields (b), the "Polar" profile.

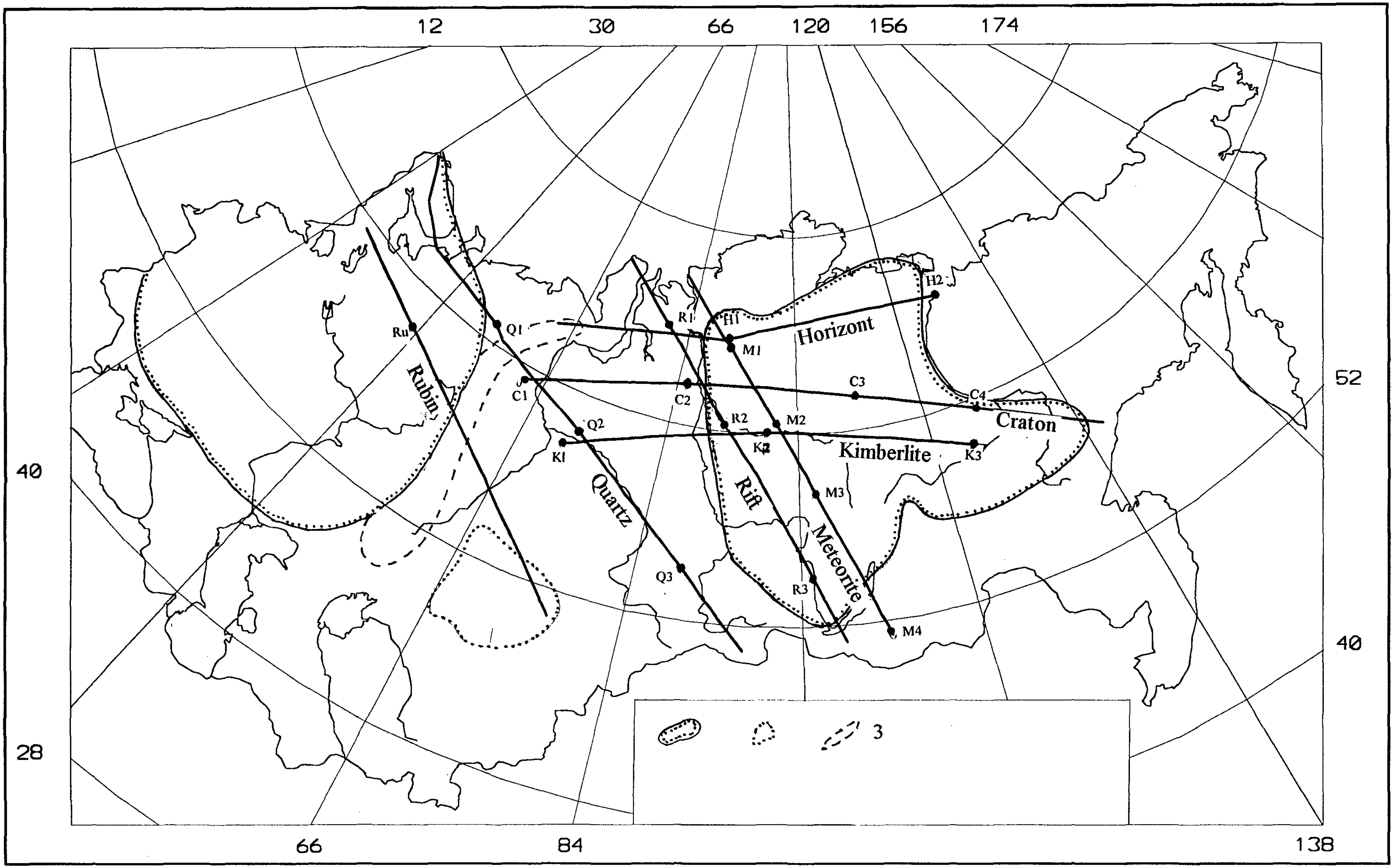
12
30
66
120
156
174
52
40
40
28
66
84
138
Rubin
Ru
Q1
C1
Q2
K1
Quartz
Q3
R1
H1
M1
Horizont
H2
C2
C3
C4
Craton
R2
M2
K2
Kimberlite
K3
Rift
M3
Meteorite
R3
M4
3

Fig. 1

"Craton", SP C1

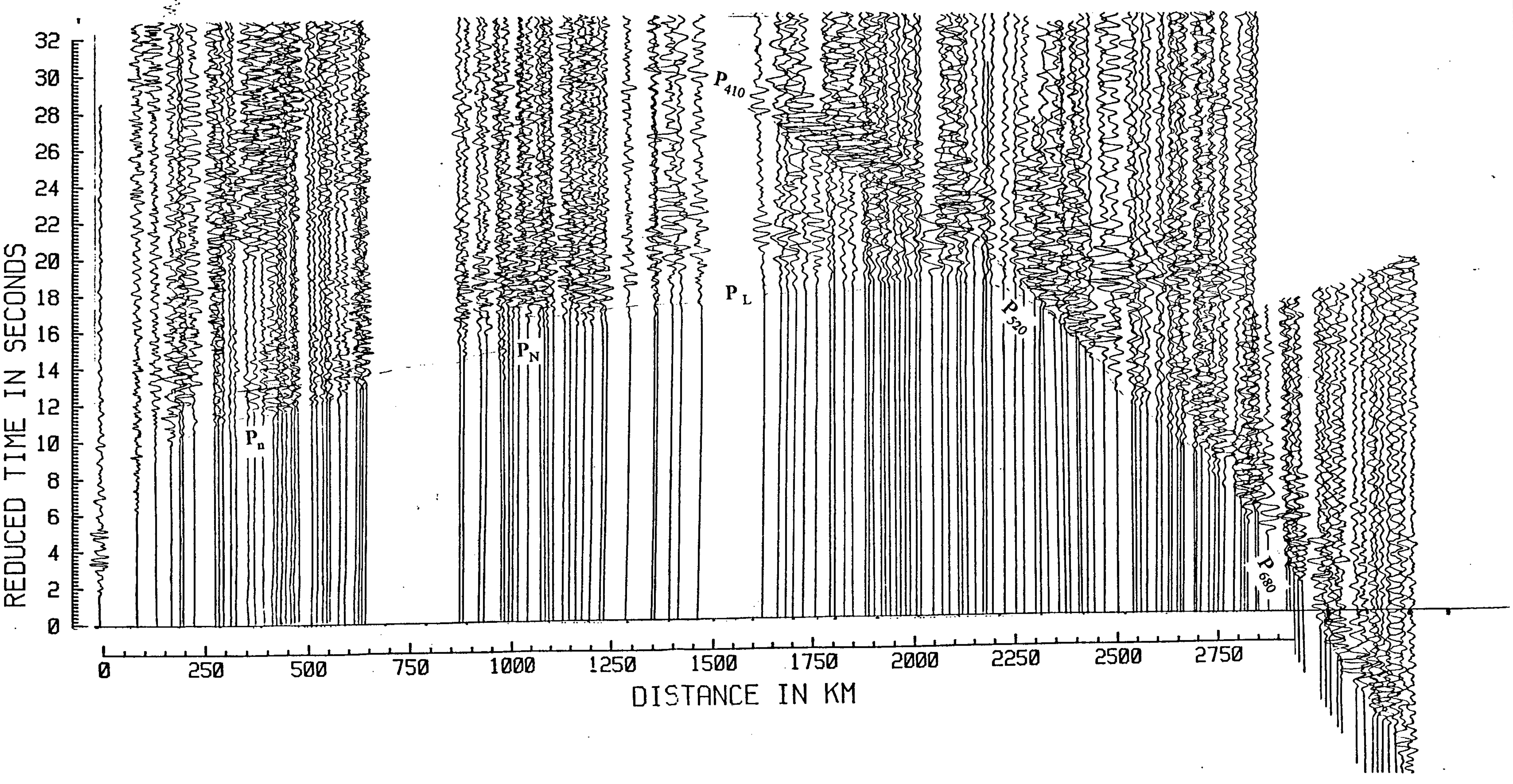

Fig. 8

Cy

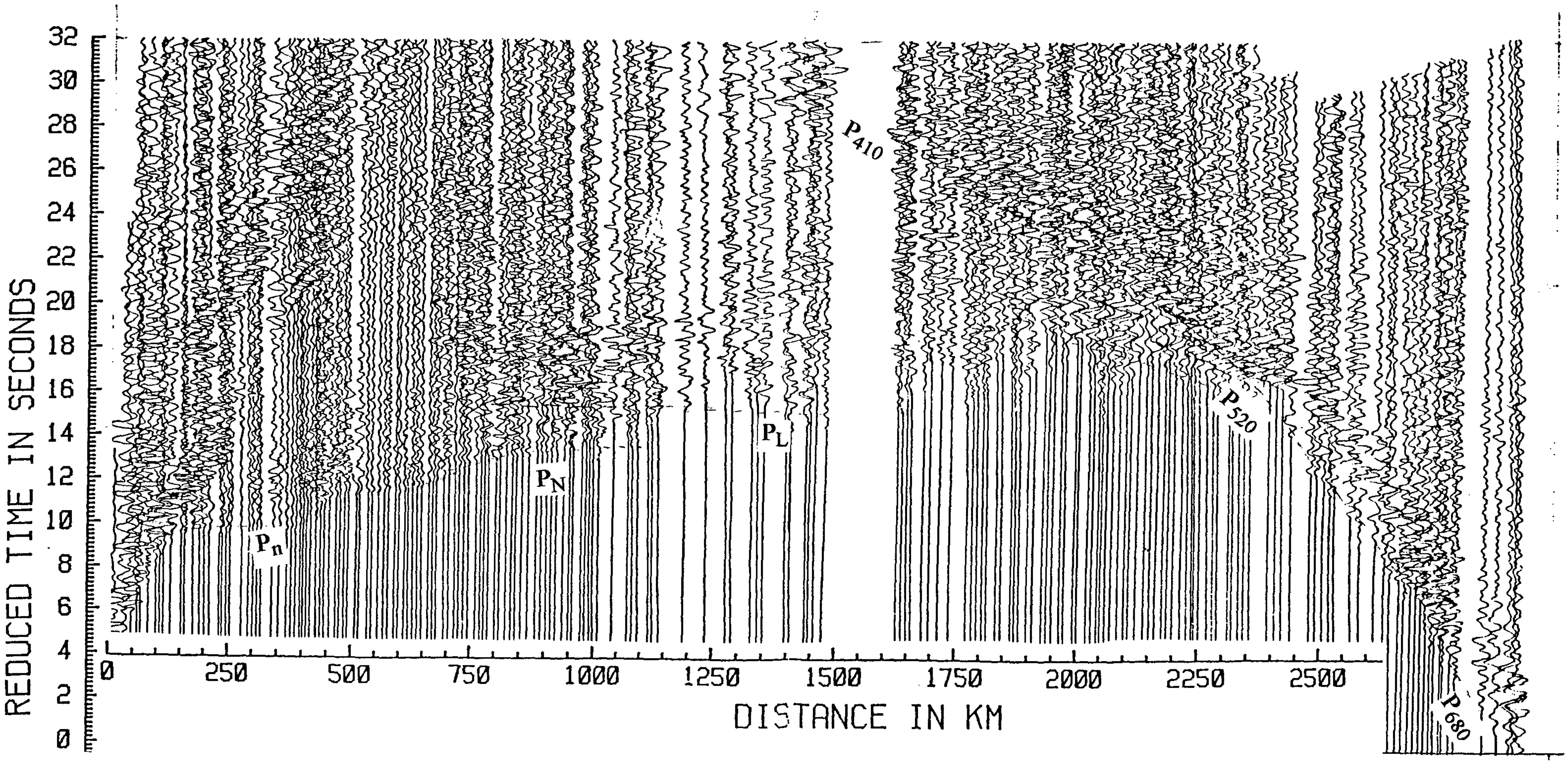

REDUCED TIME IN SECONDS
32
30
28
26
24
22
20
18
16
14
12
10
8
6
4
2
0
0
250
500
750
1000
1250
1500
1750
2000
2250
2500
DISTANCE IN KM
P_n
P_N
P_L
P_{410}
P_{520}
P_{680}

Fig. 3

44

RUSSIAN DATA QUARTZ PROFILE NORTHERN SHOT

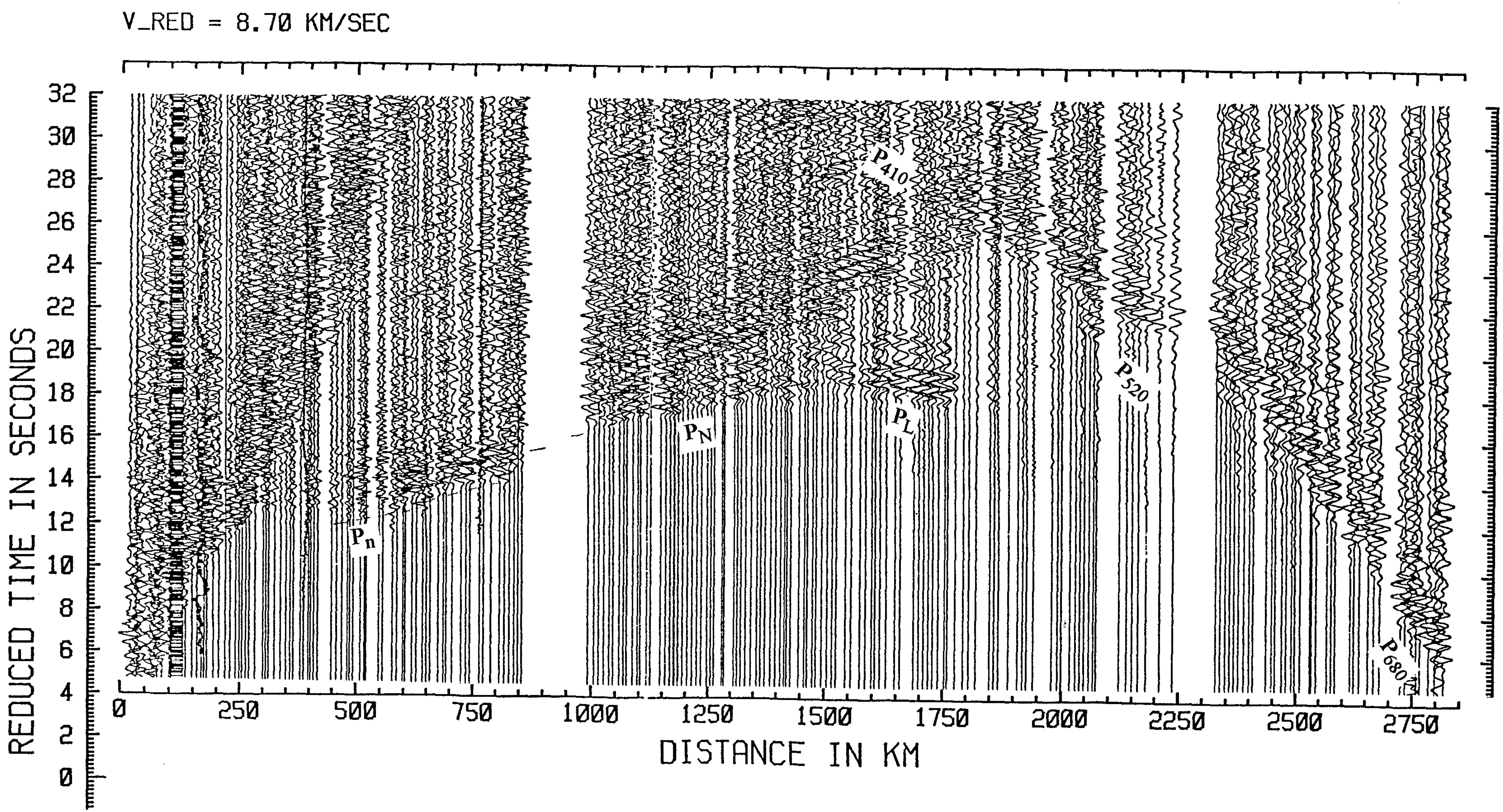

Рис. 4

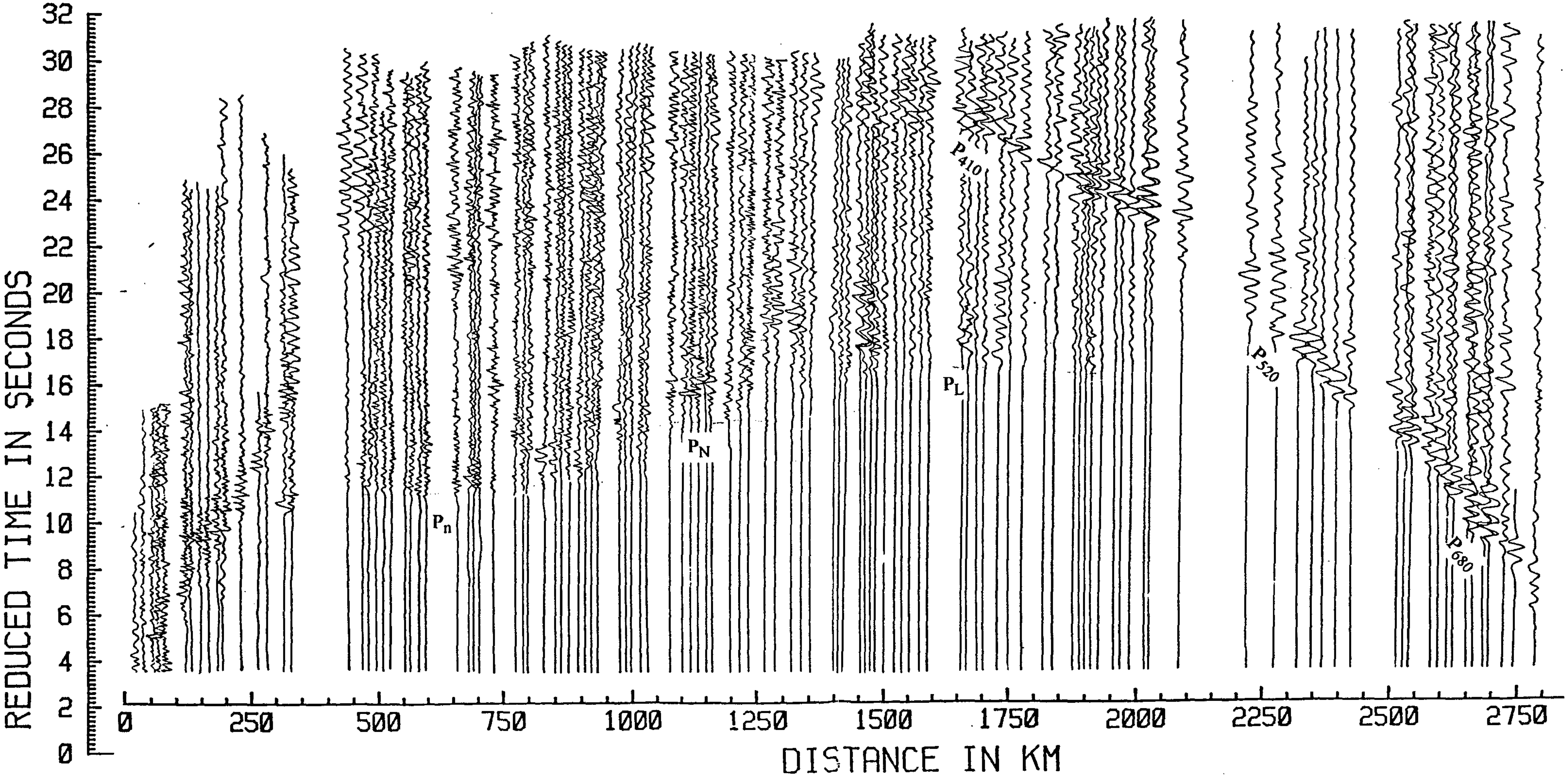
REDUCED TIME IN SECONDS
0
2
4
6
8
10
12
14
16
18
20
22
24
26
28
30
32
DISTANCE IN KM
0
250
500
750
1000
1250
1500
1750
2000
2250
2500
2750
P_n
P_N
P_L
P_{410}
P_{520}
P_{680}

Fig. 5

RECORD-SECTION for the NUCLEAR EXPLOSION C2
on the CRATON profile

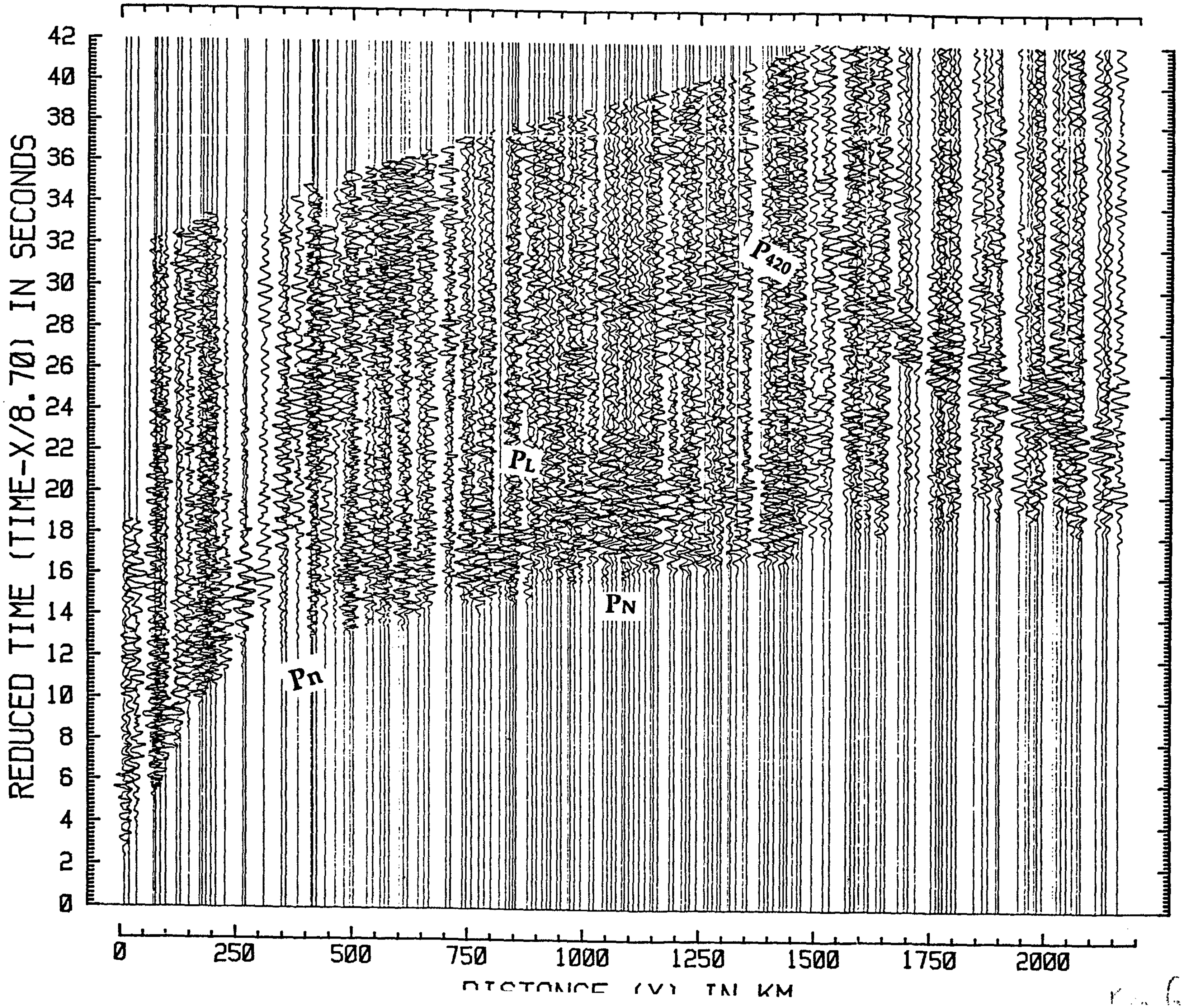

Fig.6

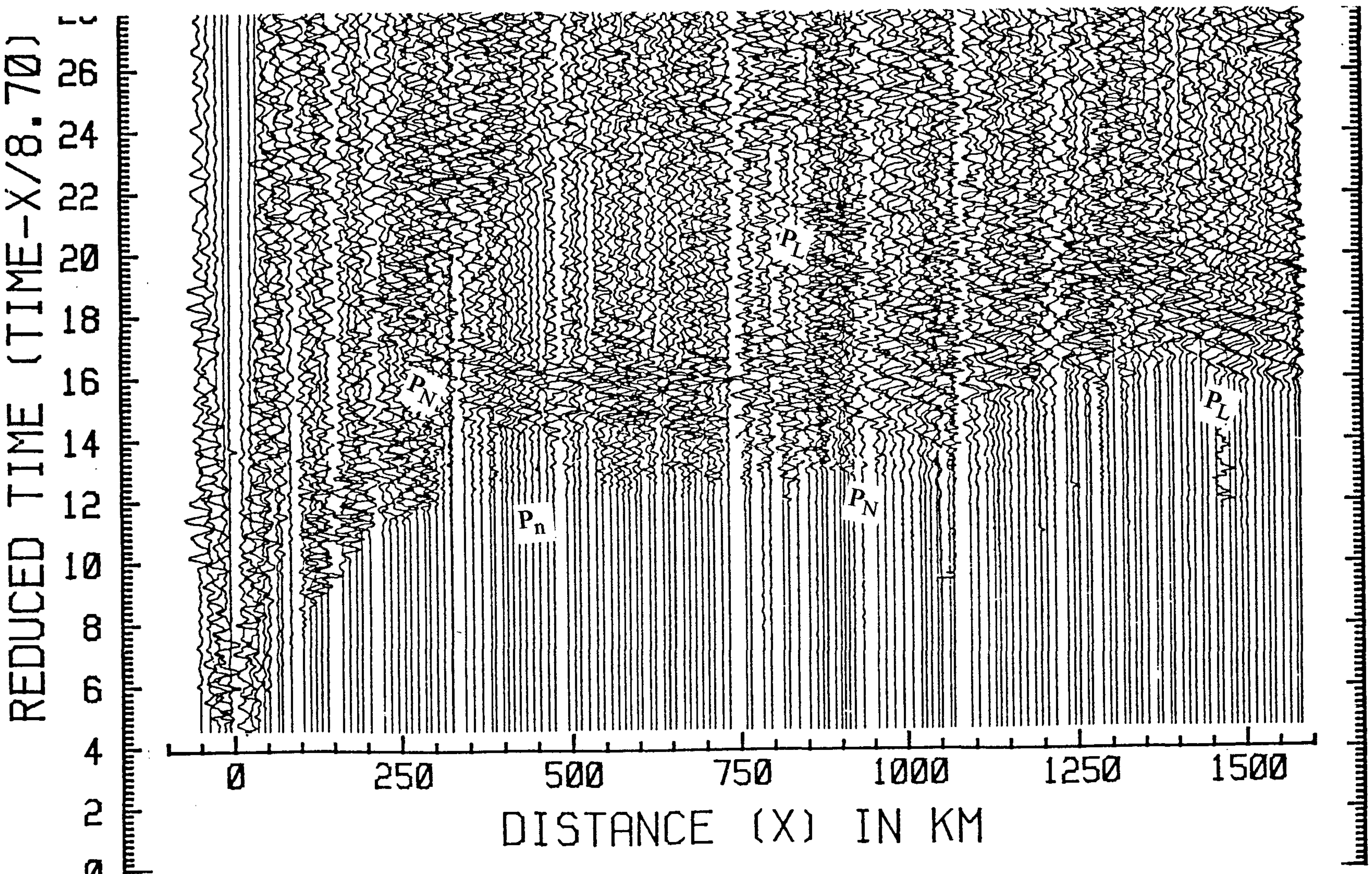

REDUCED TIME (TIME-X/8.70)
0
2
4
6
8
10
12
14
16
18
20
22
24
26
0
250
500
750
1000
1250
1500
DISTANCE (X) IN KM
P_N
P_n
P_L
P_N
P_L

Fig. 7

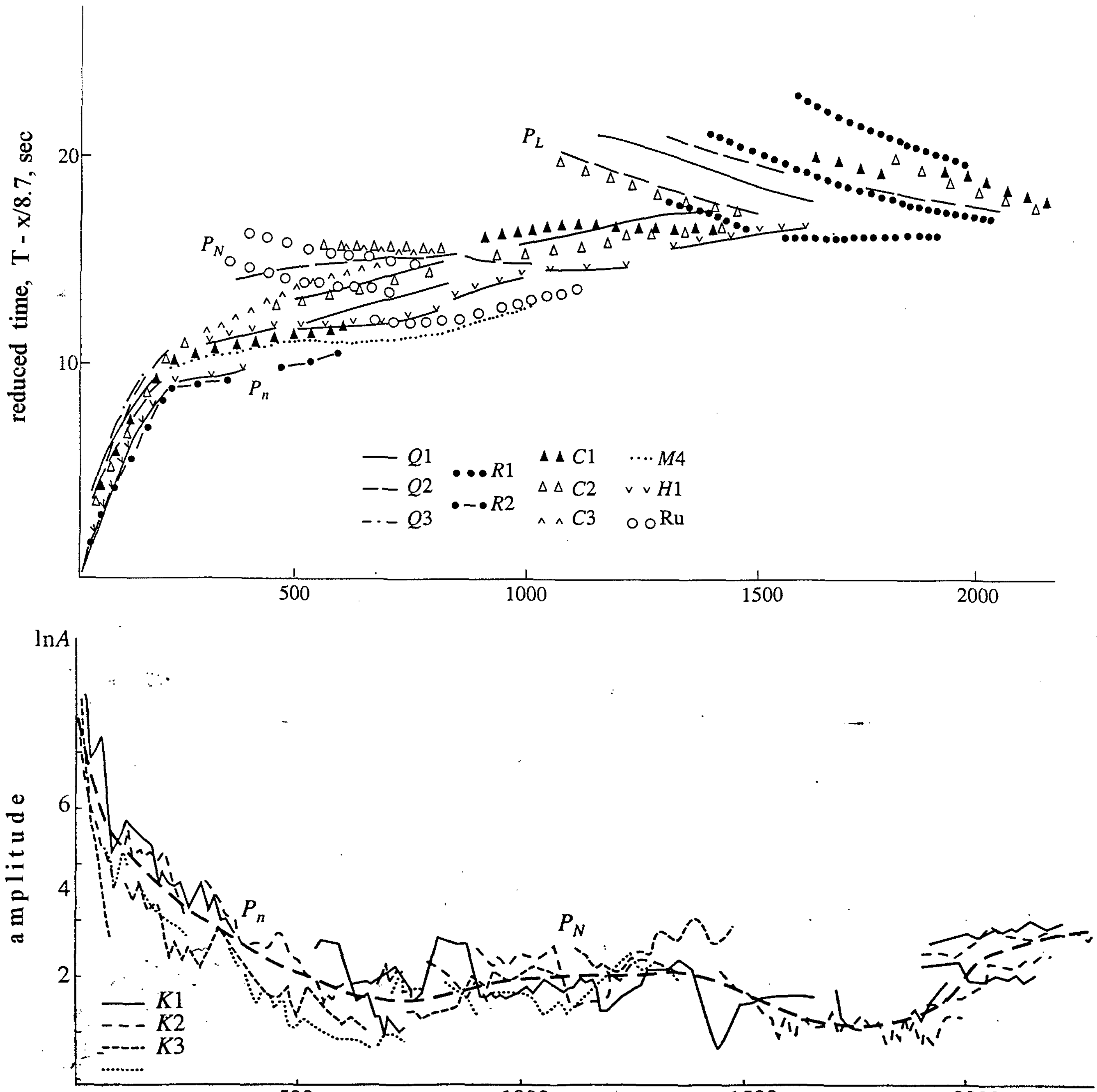

reduced time, T - x/8.7, sec
20
10
P_L
P_N
P_n
Q1
Q2
Q3
R1
R2
C1
C2
C3
M4
H1
Ru
500
1000
1500
2000
lnA
amplitude
6
4
2
P_n
P_N
K1
K2
K3
500
1000
1500
2000
distance, km

Fig. 8

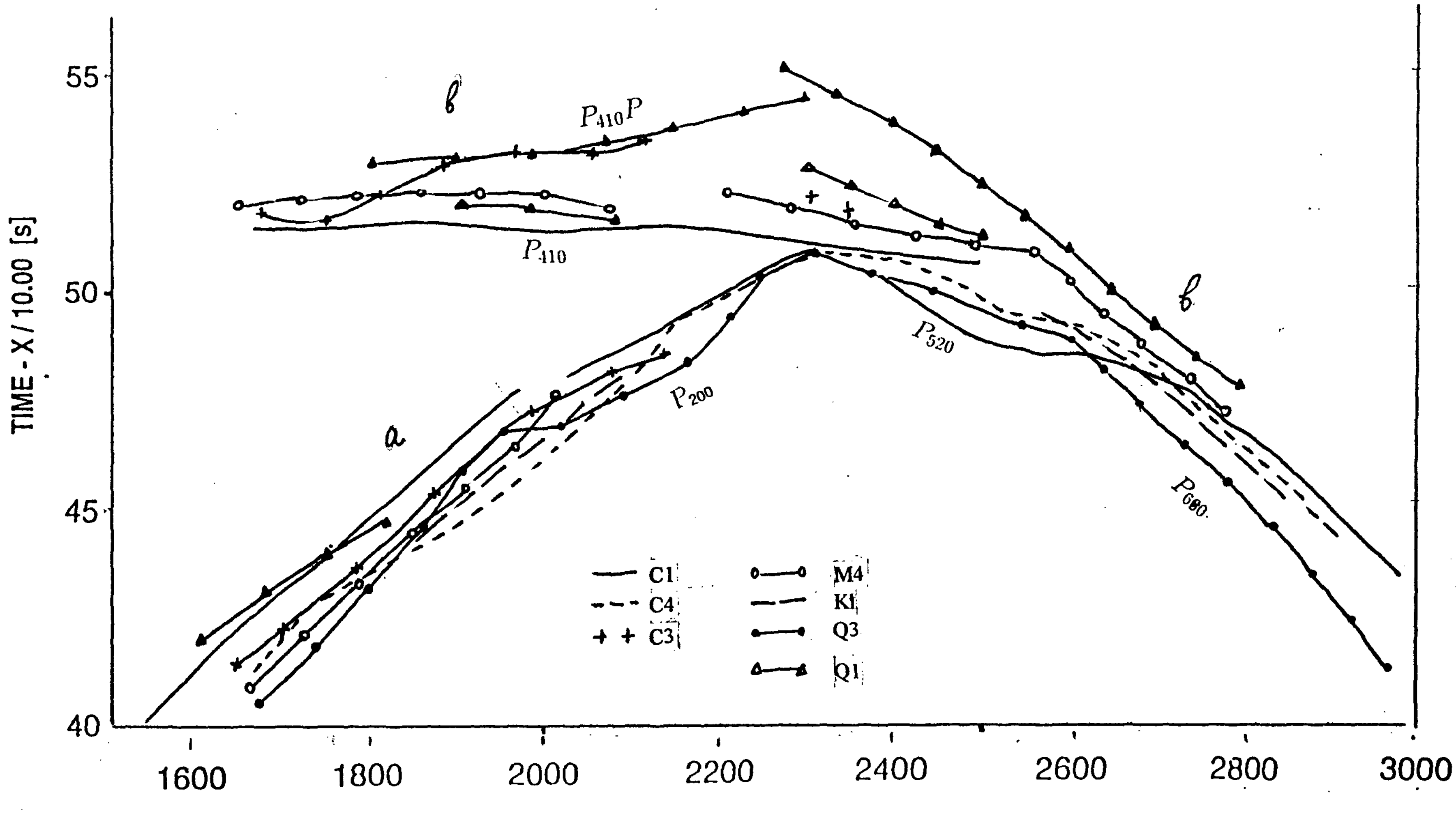

TIME - X / 10.00 [s]
55
50
45
40
1600
1800
2000
2200
2400
2600
2800
3000
b
a
$P_{410}P$
P_{410}
P_{200}
P_{520}
P_{680}
C1
C4
+ + C3
M4
K1
Q3
Q1

Fig. 9

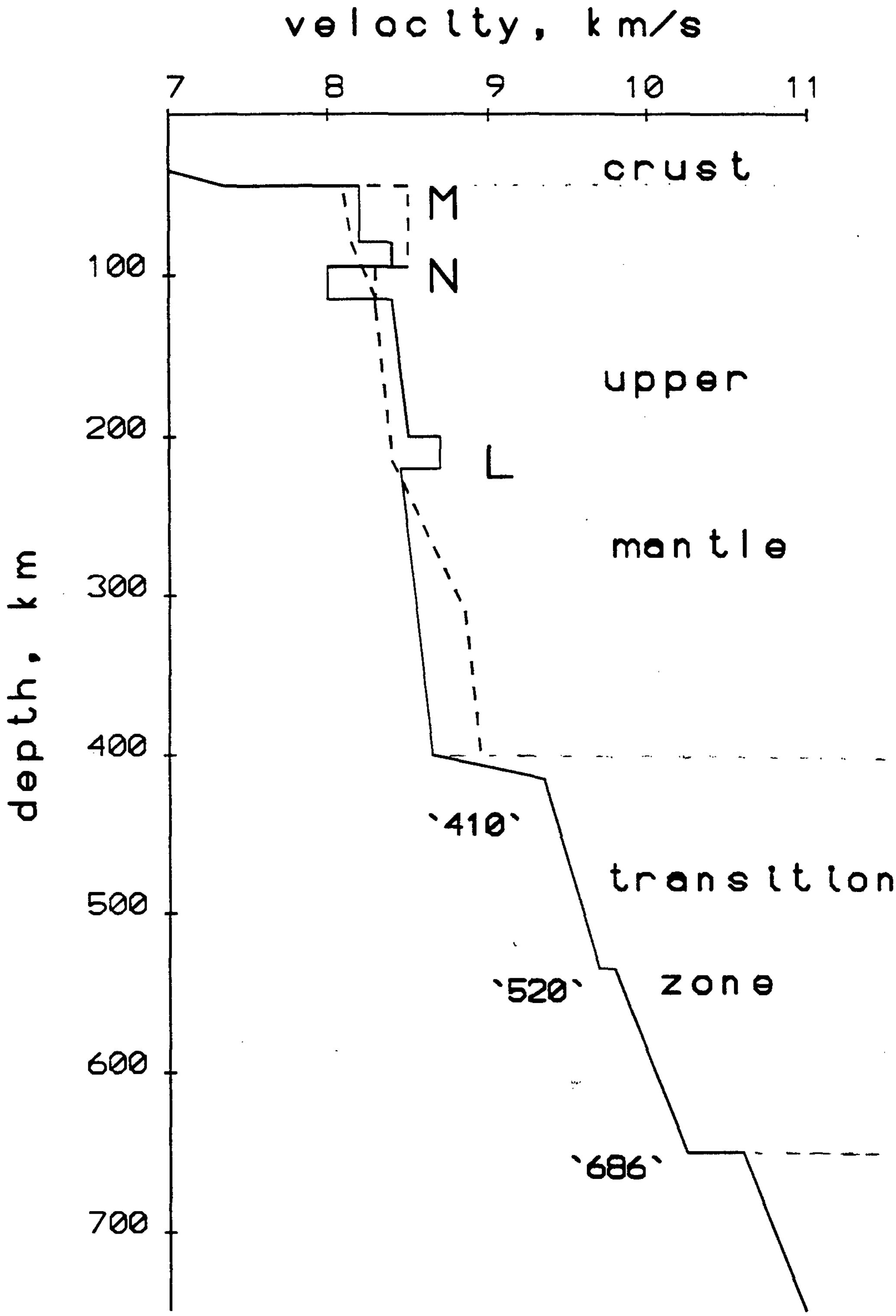
velocity, km/s
7
8
9
10
11
crust
M
N
upper
L
mantle
transition
zone
100
200
300
400
500
600
700
depth, km
`410`
`520`
`686`

Fig. 10

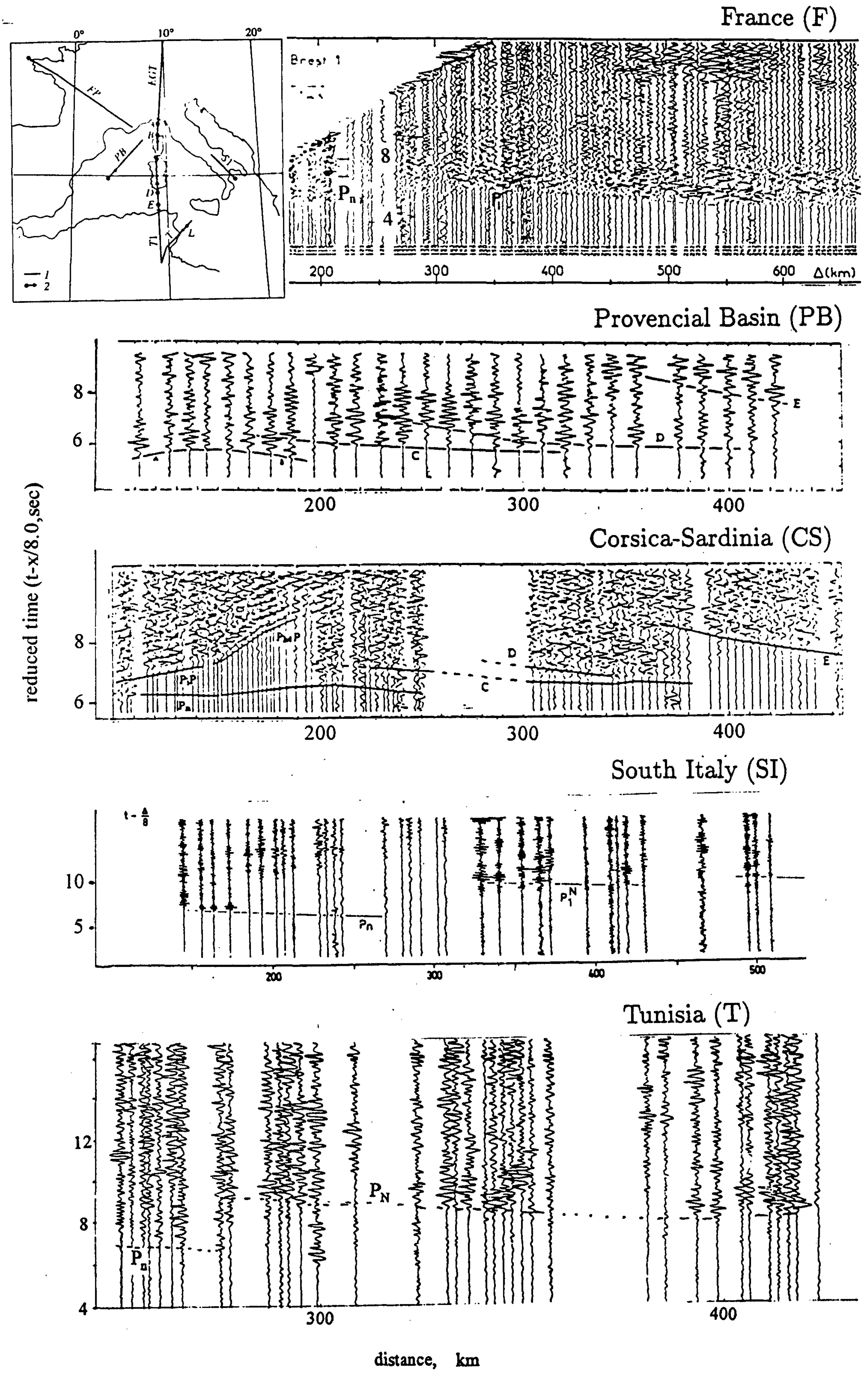
France (F)
0°
10°
20°
FP
EGT
PB
SI
D
E
TI
L
1
2
Brest 1
8
4
Pn
200
300
400
500
600
Δ(km)
Provencial Basin (PB)
8
6
A
B
C
D
E
200
300
400
Corsica-Sardinia (CS)
reduced time (t-x/8.0,sec)
8
6
PmP
PiP
Pn
D
C
E
200
300
400
South Italy (SI)
t - Δ/8
10
5
Pn
P1N
200
300
400
500
Tunisia (T)
12
8
4
PN
Pn
300
400
distance, km

Fig. 11

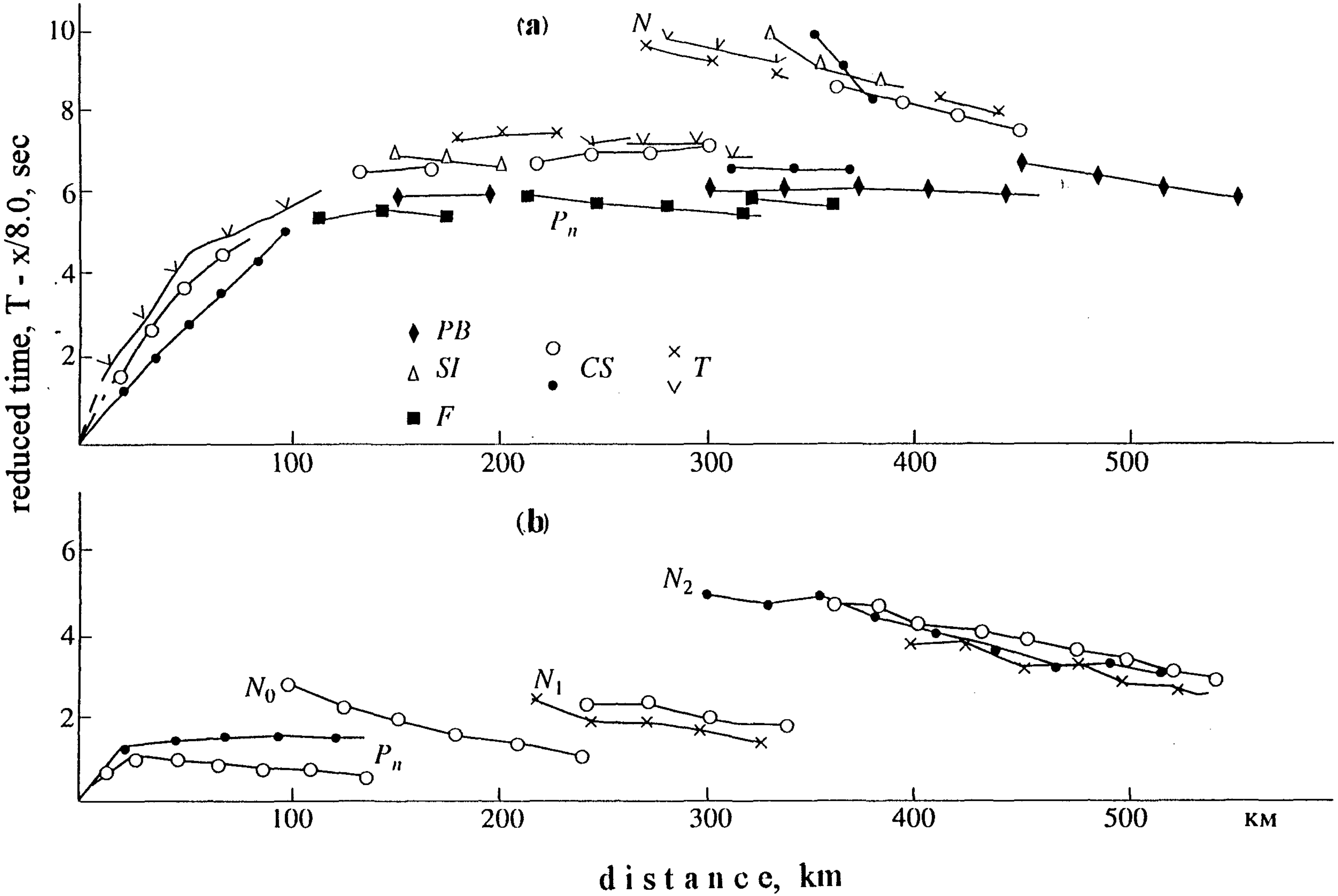
(a)
(b)
N
P_n
PB
SI
F
CS
T
N_0
N_1
N_2
10
8
6
4
2
100
200
300
400
500
км
reduced time, T - x/8.0, sec
distance, km

Fig.12

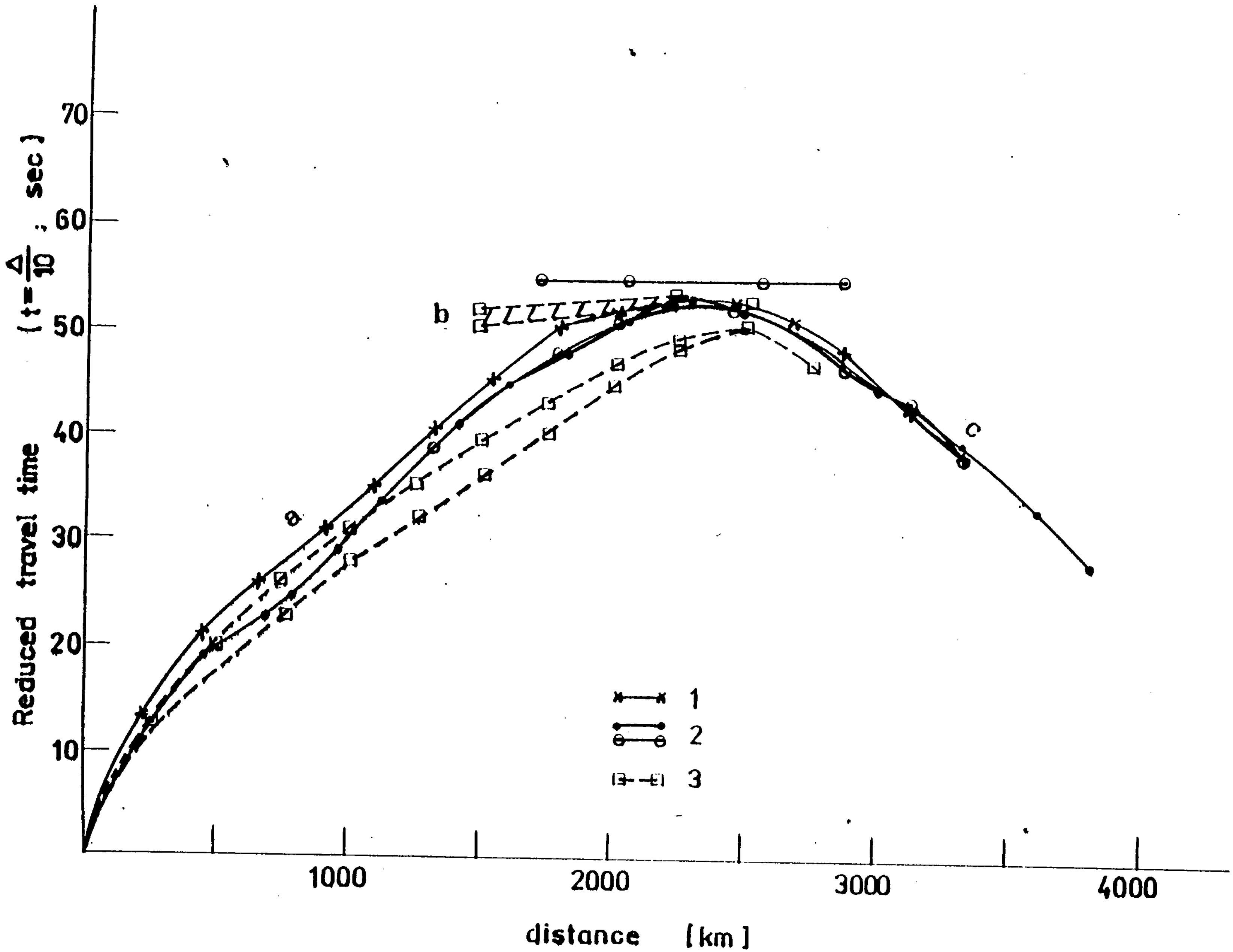
Reduced travel time
(t = Δ/10 ; sec)
70
60
50
40
30
20
10
1000
2000
3000
4000
distance [km]
a
b
c
1
2
3

Fig. 13

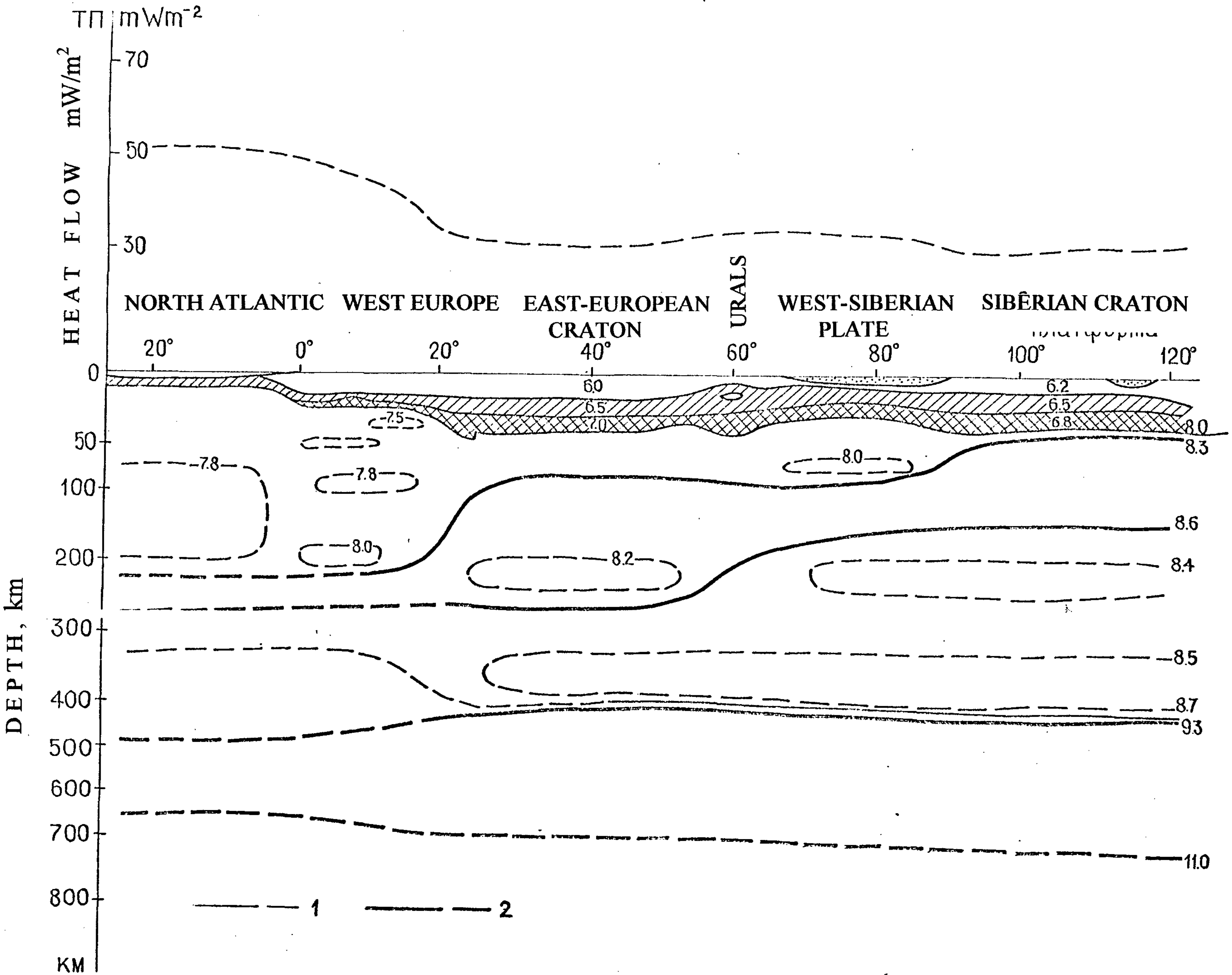

ТП mWm-2
HEAT FLOW mW/m2
70
50
30
NORTH ATLANTIC
WEST EUROPE
EAST-EUROPEAN CRATON
URALS
WEST-SIBERIAN PLATE
SIBÊRIAN CRATON
20°
0°
20°
40°
60°
80°
100°
120°
DEPTH, km
0
50
100
200
300
400
500
600
700
800
KM
6.0
6.5
7.0
6.2
6.5
6.8
7.5
7.8
7.8
8.0
8.0
8.0
8.2
8.3
8.6
8.4
8.5
8.7
9.3
11.0
1
2

Fig. 14

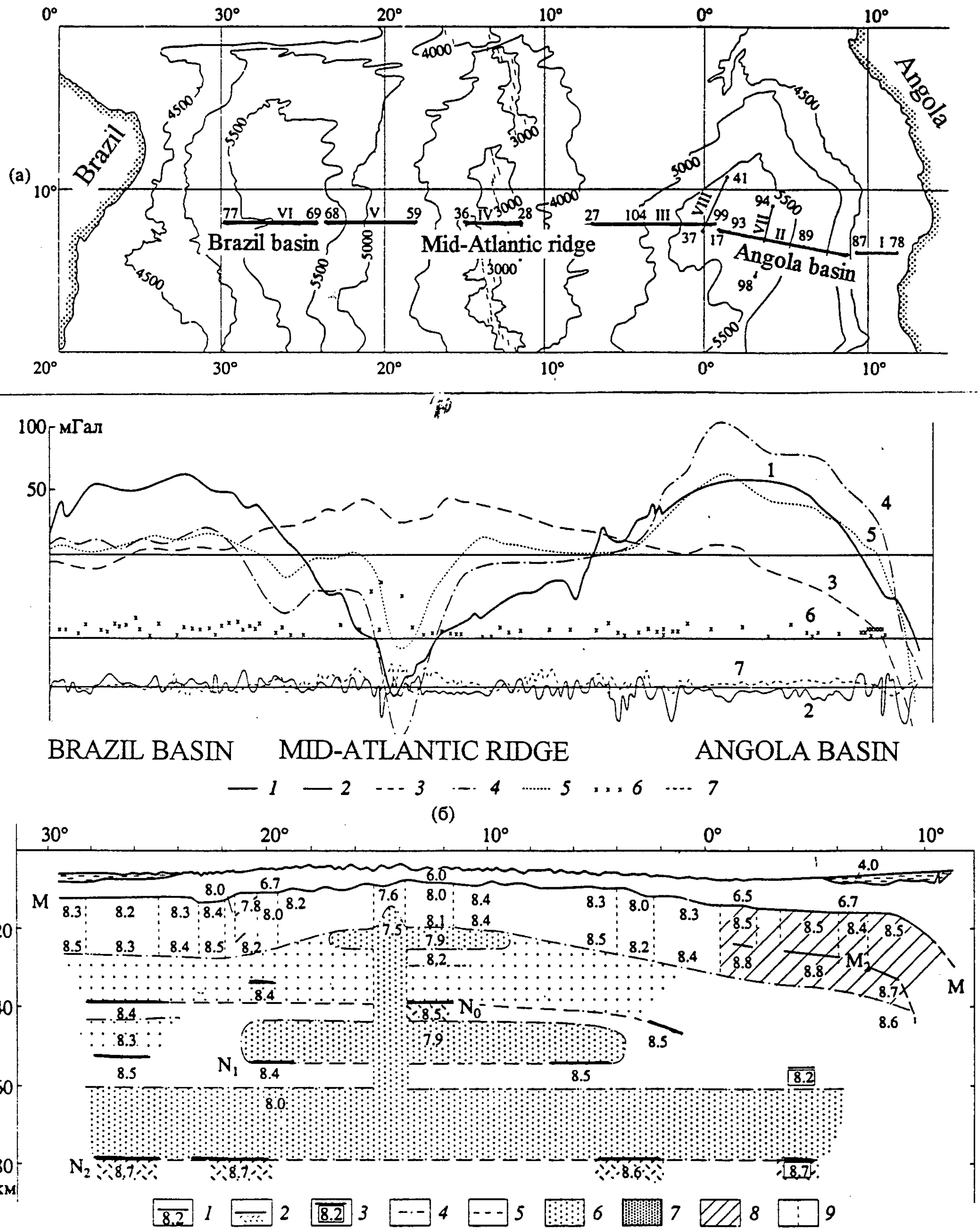
(a)
Brazil
Angola
Brazil basin
Mid-Atlantic ridge
Angola basin
100 мГал
BRAZIL BASIN
MID-ATLANTIC RIDGE
ANGOLA BASIN
— 1 — 2 --- 3 -·- 4 ····· 5 x x x 6 ---- 7
(б)
км
1 2 3 4 5 6 7 8 9

Fig. 15

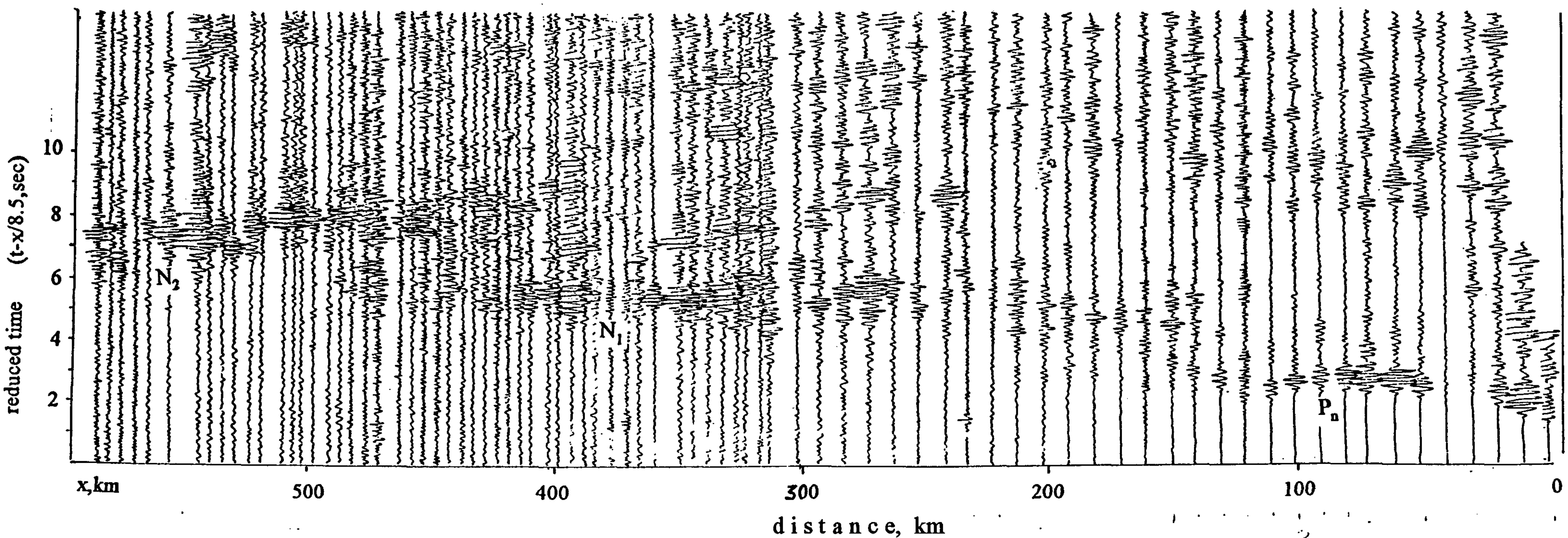
reduced time (t-x/8.5,sec)
10
8
6
4
2
x,km
500
400
300
200
100
0
distance, km
P_n
N_1
N_2

Fig. 16

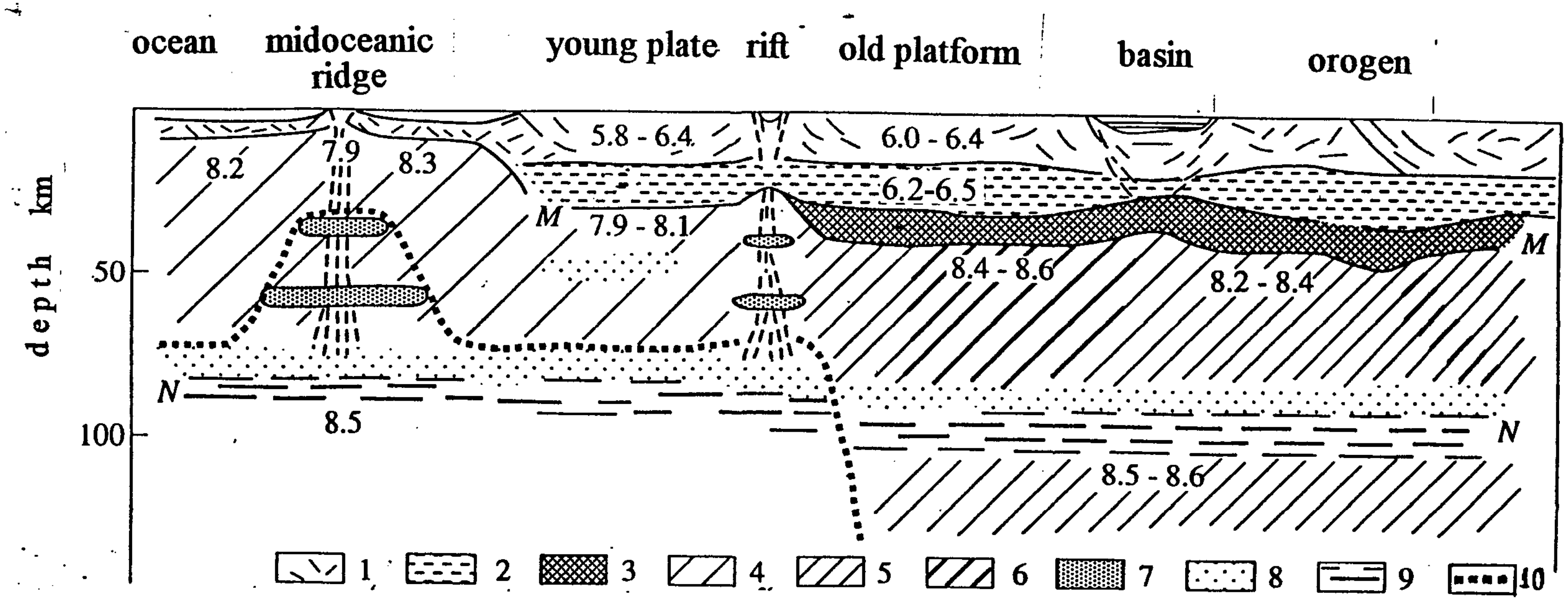
ocean
midoceanic ridge
young plate
rift
old platform
basin
orogen
depth km
50
100
8.2
7.9
8.3
5.8 - 6.4
6.0 - 6.4
6.2-6.5
M
7.9 - 8.1
8.4 - 8.6
8.2 - 8.4
N
8.5
8.5 - 8.6
1
2
3
4
5
6
7
8
9
10

Fig. 17

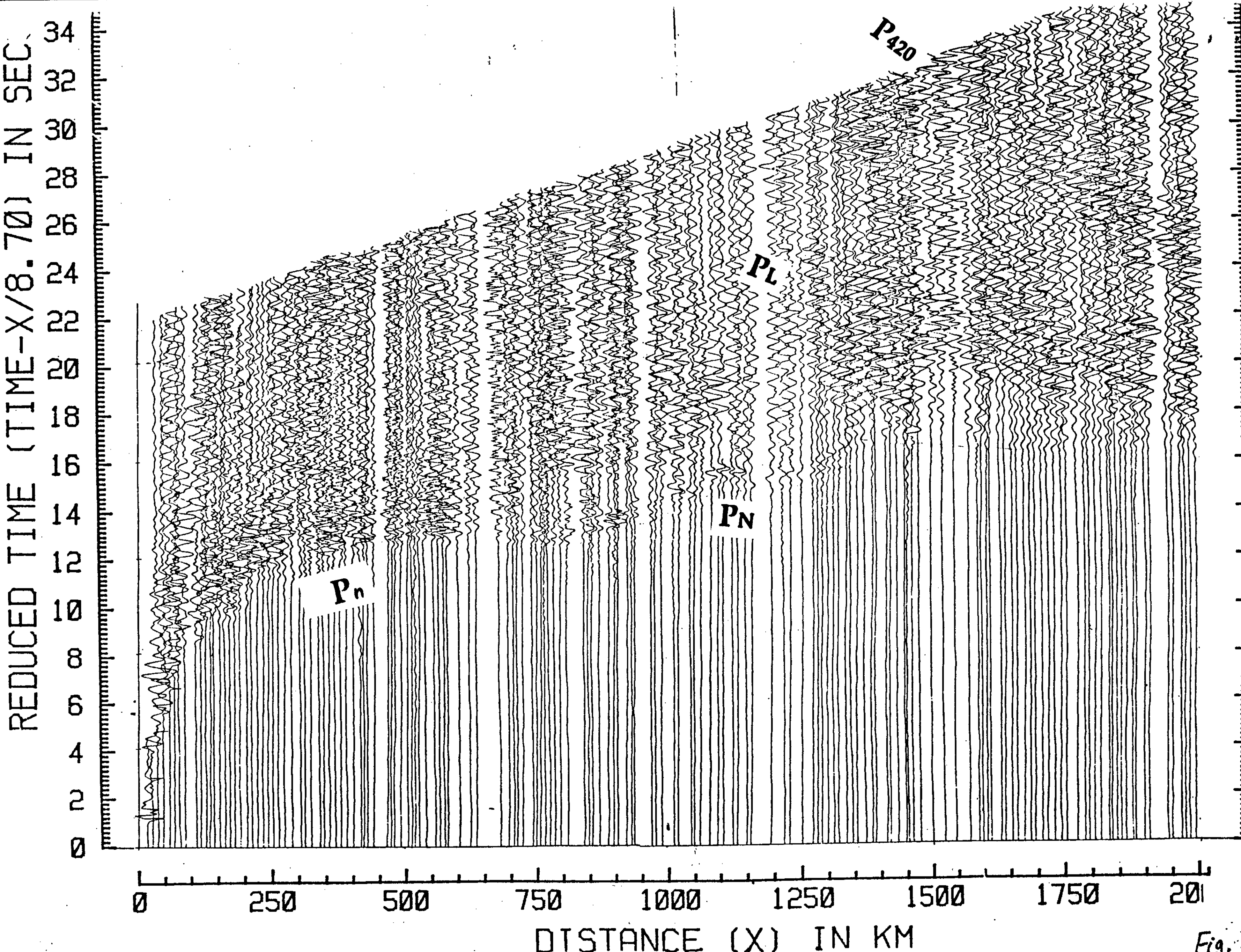

REDUCED TIME (TIME-X/8.70) IN SEC.
34
32
30
28
26
24
22
20
18
16
14
12
10
8
6
4
2
0
0
250
500
750
1000
1250
1500
1750
201
DISTANCE (X) IN KM
P_{420}
P_L
P_N
P_n

Fig. 18

RECORD-SECTION for the NUCLEAR EXPLOSION R2 on the RIFT profile

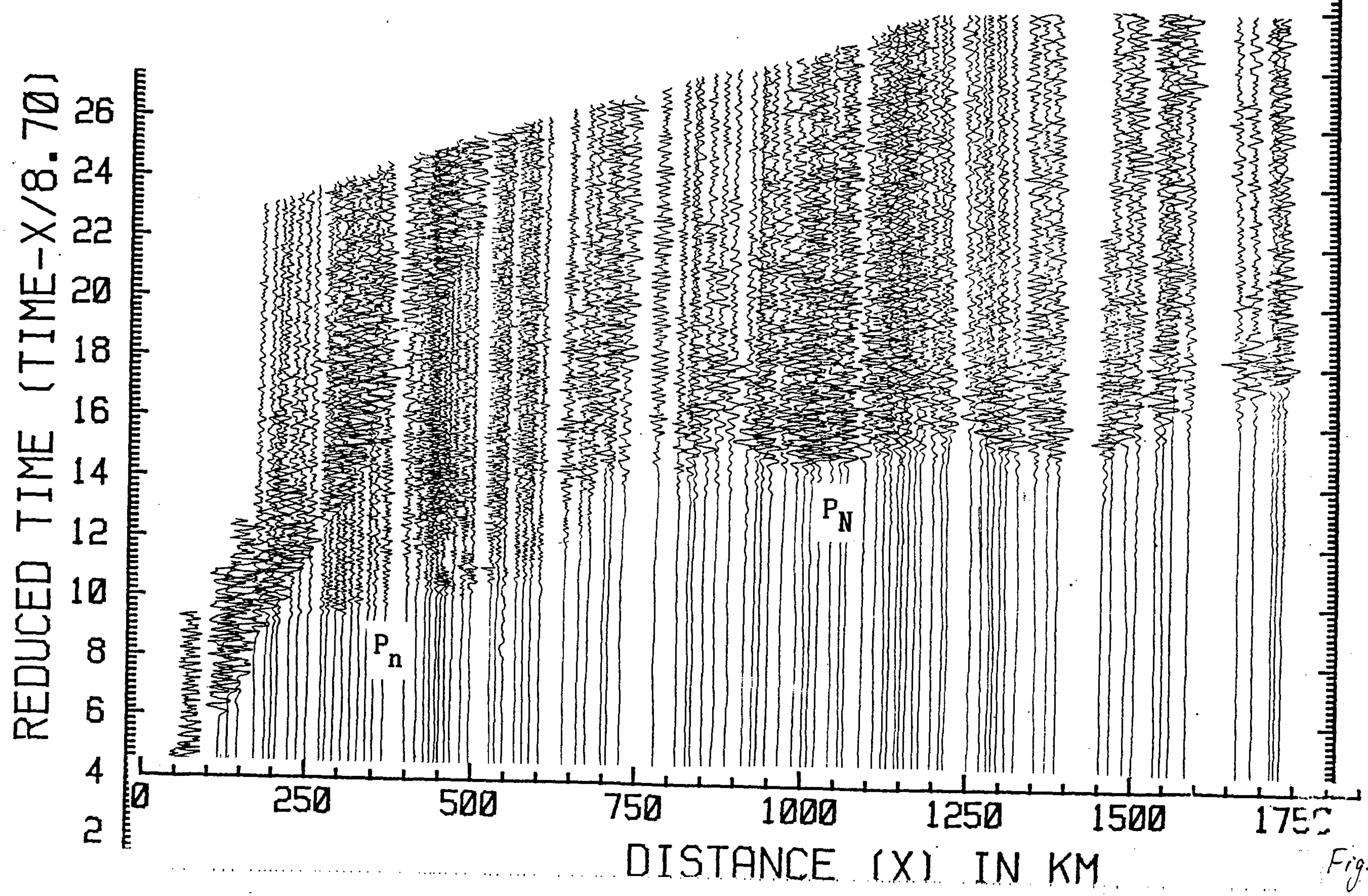

Fig. 19

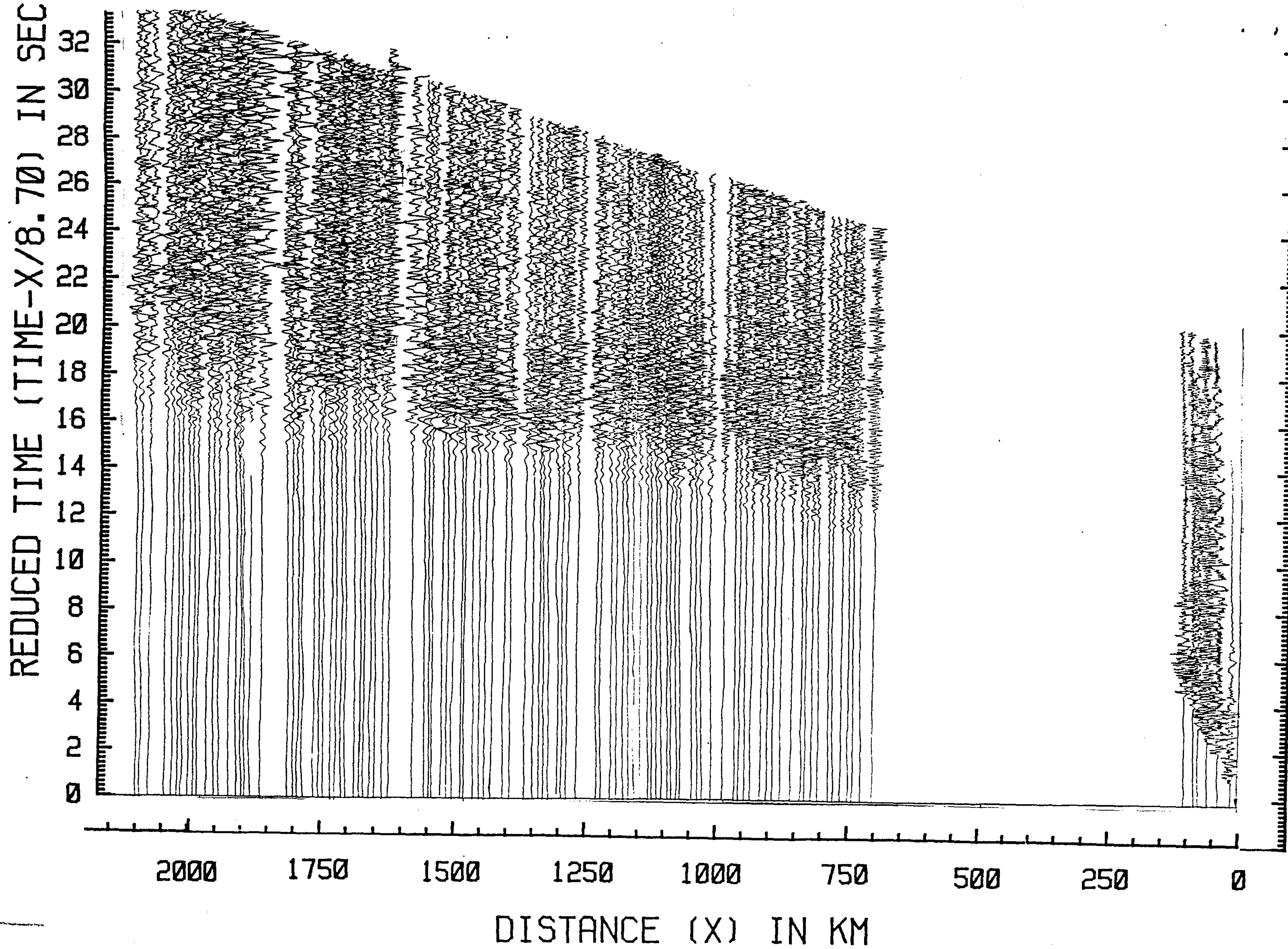
REDUCED TIME (TIME-X/8.70) IN SEC
32
30
28
26
24
22
20
18
16
14
12
10
8
6
4
2
0
2000
1750
1500
1250
1000
750
500
250
0
DISTANCE (X) IN KM

Fig.20

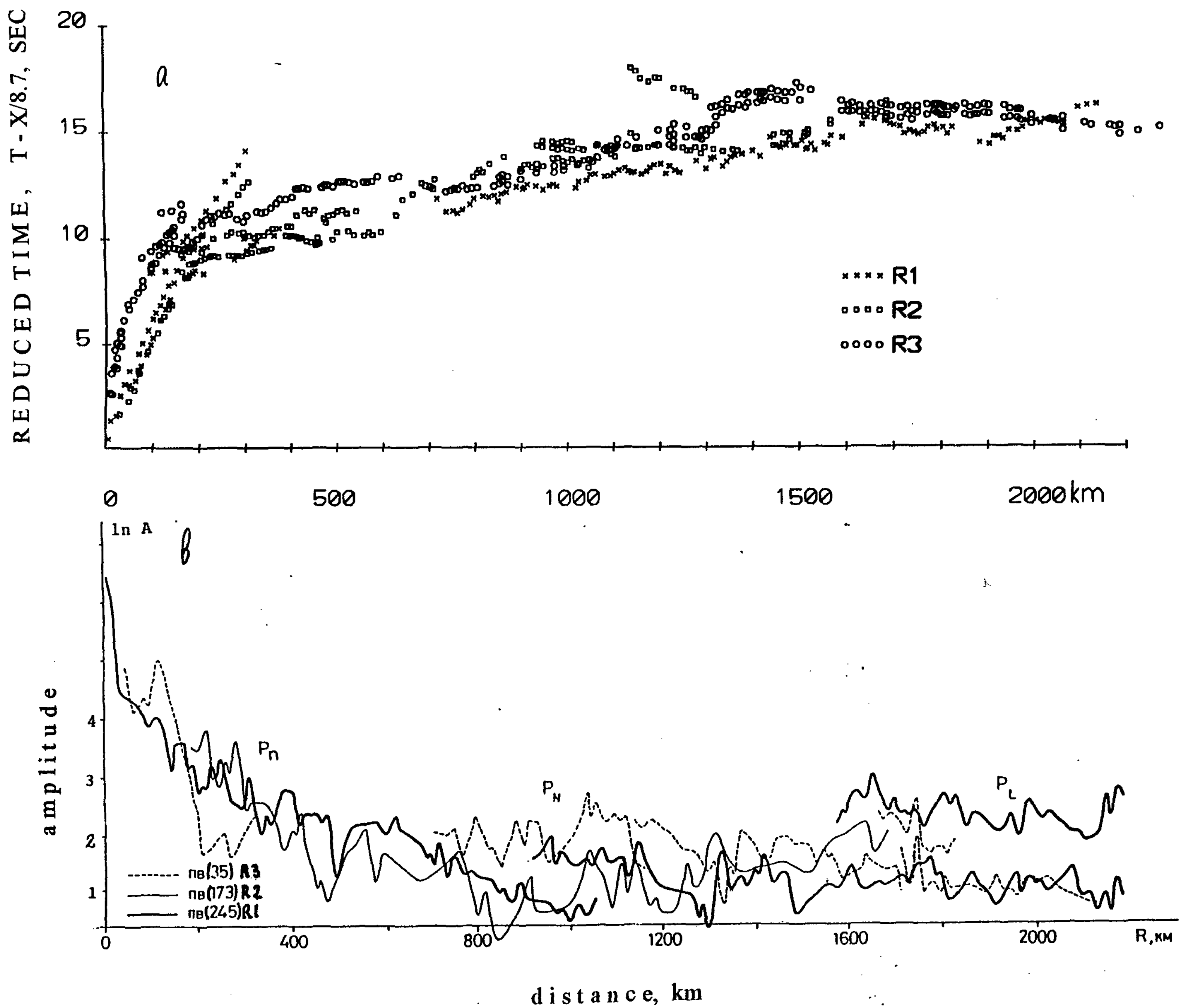
REDUCED TIME, T - X/8.7, SEC
20
15
10
5
a
R1
R2
R3
0
500
1000
1500
2000km
ln A
в
amplitude
4
3
2
1
P_n
P_N
P_L
пв(35) R3
пв(173) R2
пв(245) R1
0
400
800
1200
1600
2000
R, км
distance, km

Fig.21

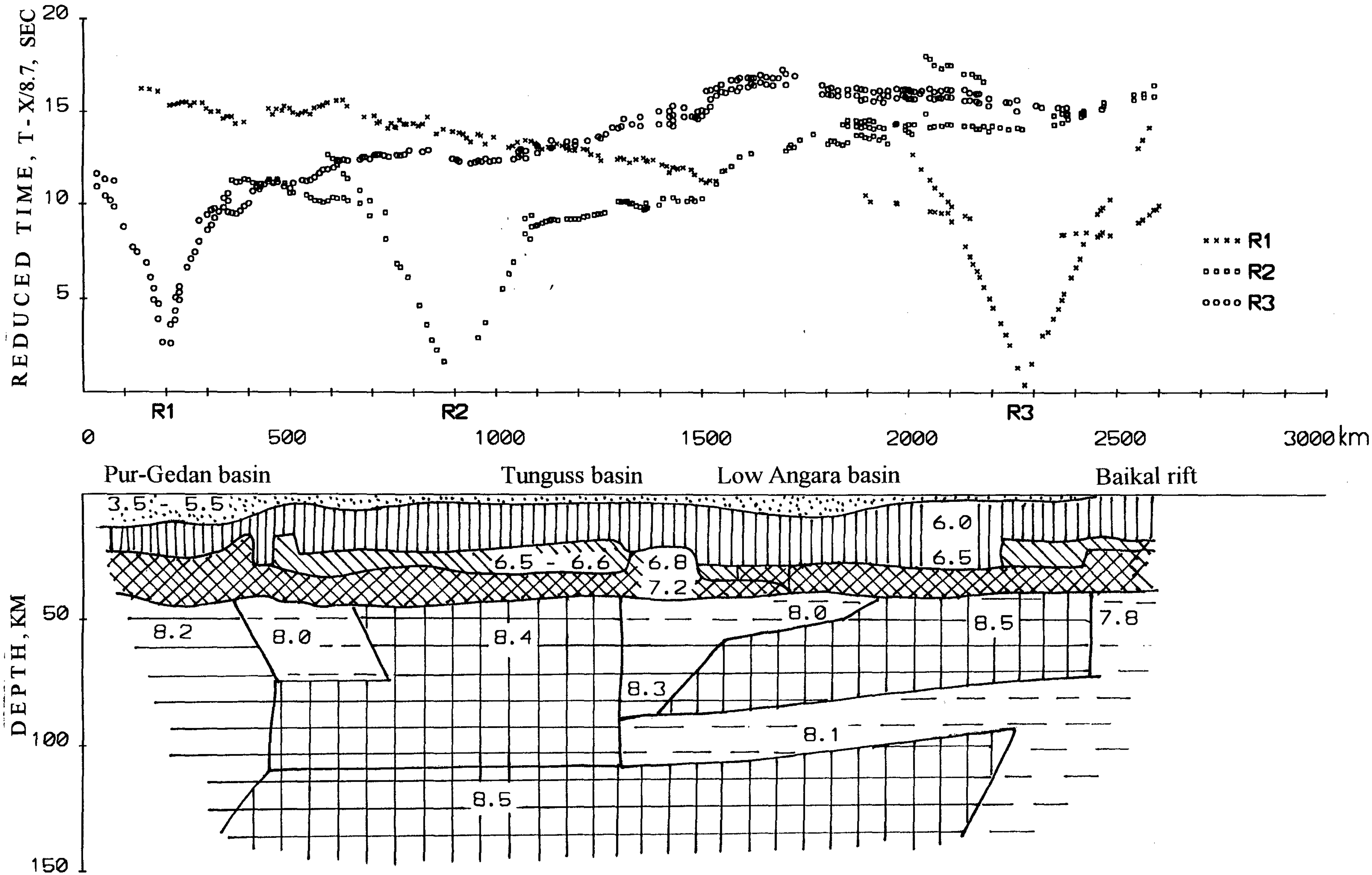
REDUCED TIME, T - X/8.7, SEC
20
15
10
5
R1
R2
R3
0
500
1000
1500
2000
2500
3000km
R1
R2
R3
Pur-Gedan basin
Tunguss basin
Low Angara basin
Baikal rift
3.5 - 5.5
6.0
6.5
6.5 - 6.6
6.8
7.2
8.2
8.0
8.4
8.0
8.5
7.8
8.3
8.1
8.5
DEPTH, KM
50
100
150

Fig.22

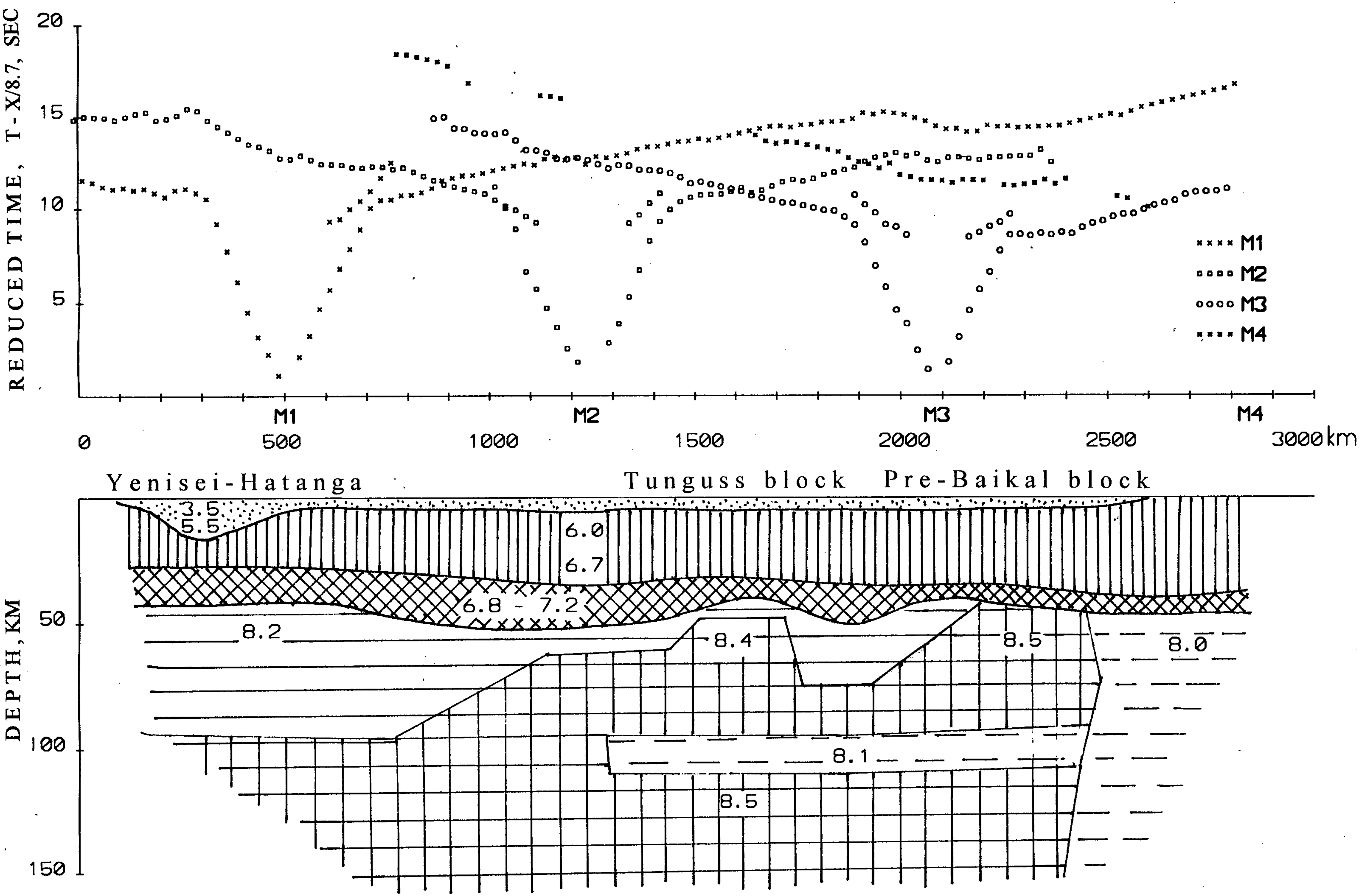

REDUCED TIME, T - X/8.7, SEC
20
15
10
5
M1
M2
M3
M4
0
500
1000
1500
2000
2500
3000km
Yenisei-Hatanga
Tunguss block
Pre-Baikal block
3.5
5.5
6.0
6.7
6.8 - 7.2
8.2
8.4
8.5
8.0
8.1
8.5
DEPTH, KM
50
100
150

Fig. 23

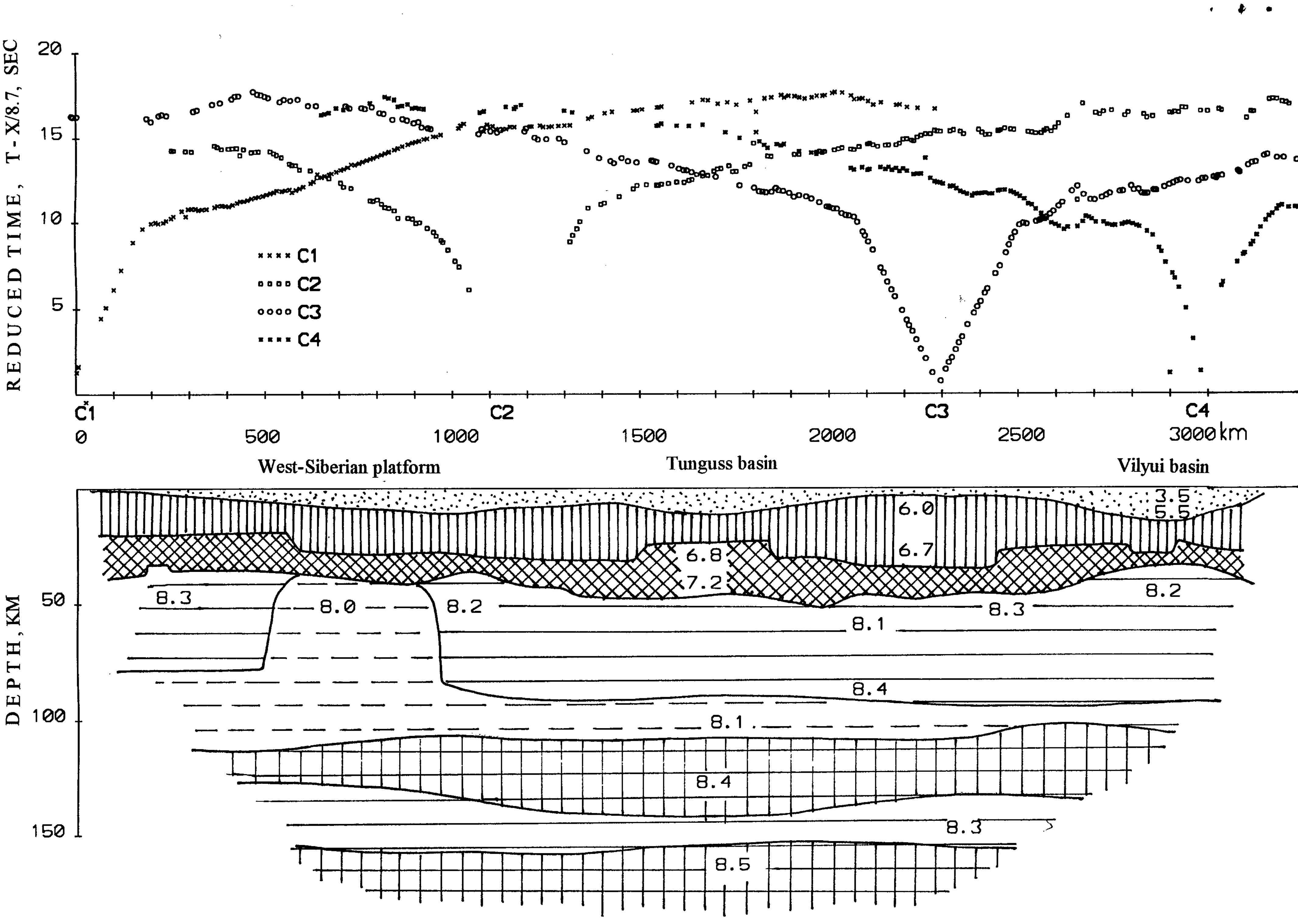
REDUCED TIME, T - X/8.7, SEC
20
15
10
5
C1
C2
C3
C4
0
500
1000
1500
2000
2500
3000 km
West-Siberian platform
Tunguss basin
Vilyui basin
DEPTH, KM
50
100
150
3.5
5.5
6.0
6.7
6.8
7.2
8.3
8.0
8.2
8.1
8.4
8.5

Fig. 24

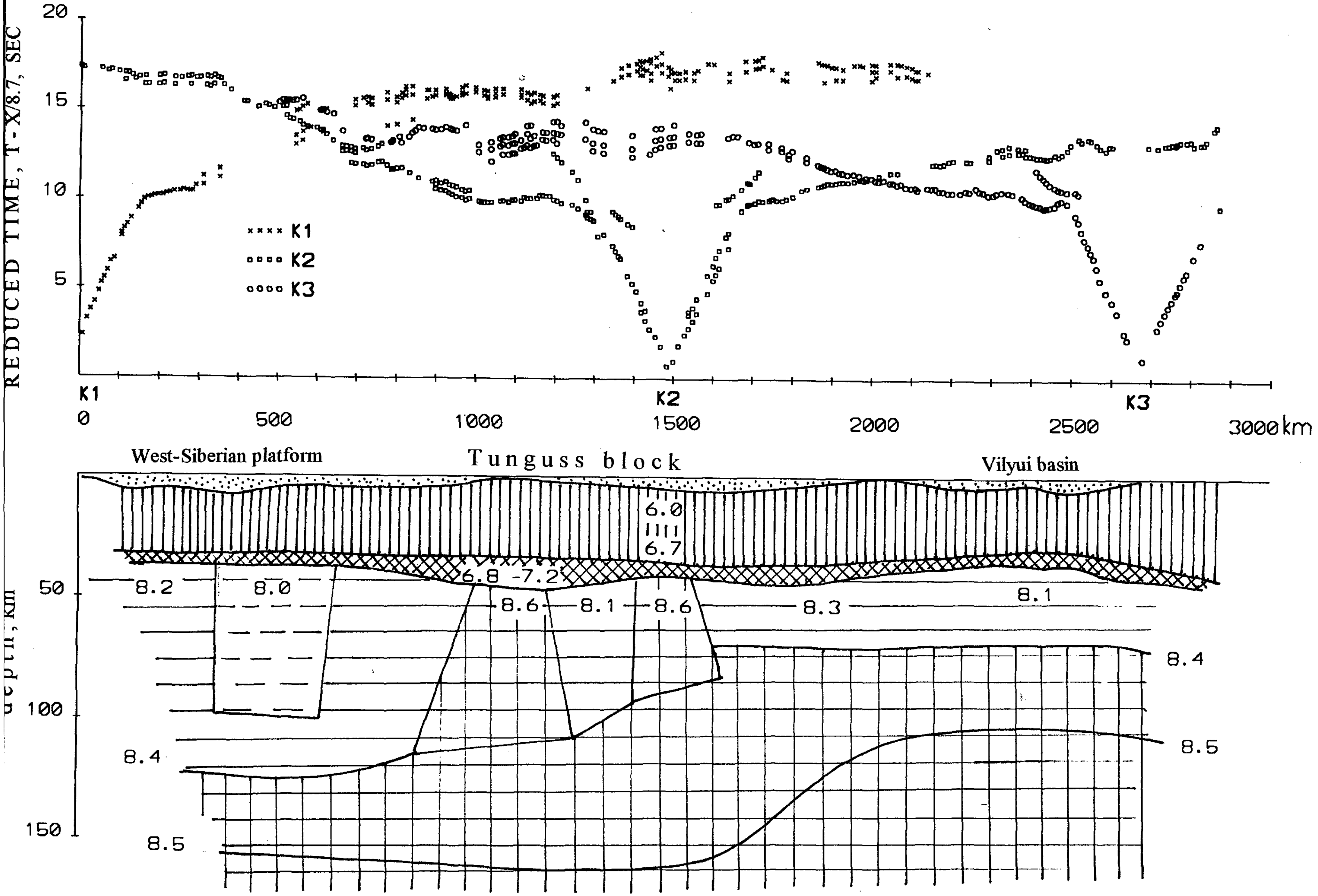

REDUCED TIME, T - X/8.7, SEC
20
15
10
5
K1
K2
K3
0
500
1000
1500
2000
2500
3000km
West-Siberian platform
Tunguss block
Vilyui basin
6.0
6.7
6.8 -7.2
8.2
8.0
8.6
8.1
8.6
8.3
8.1
8.4
8.5
8.4
8.5
depth, km
50
100
150

Fig.25

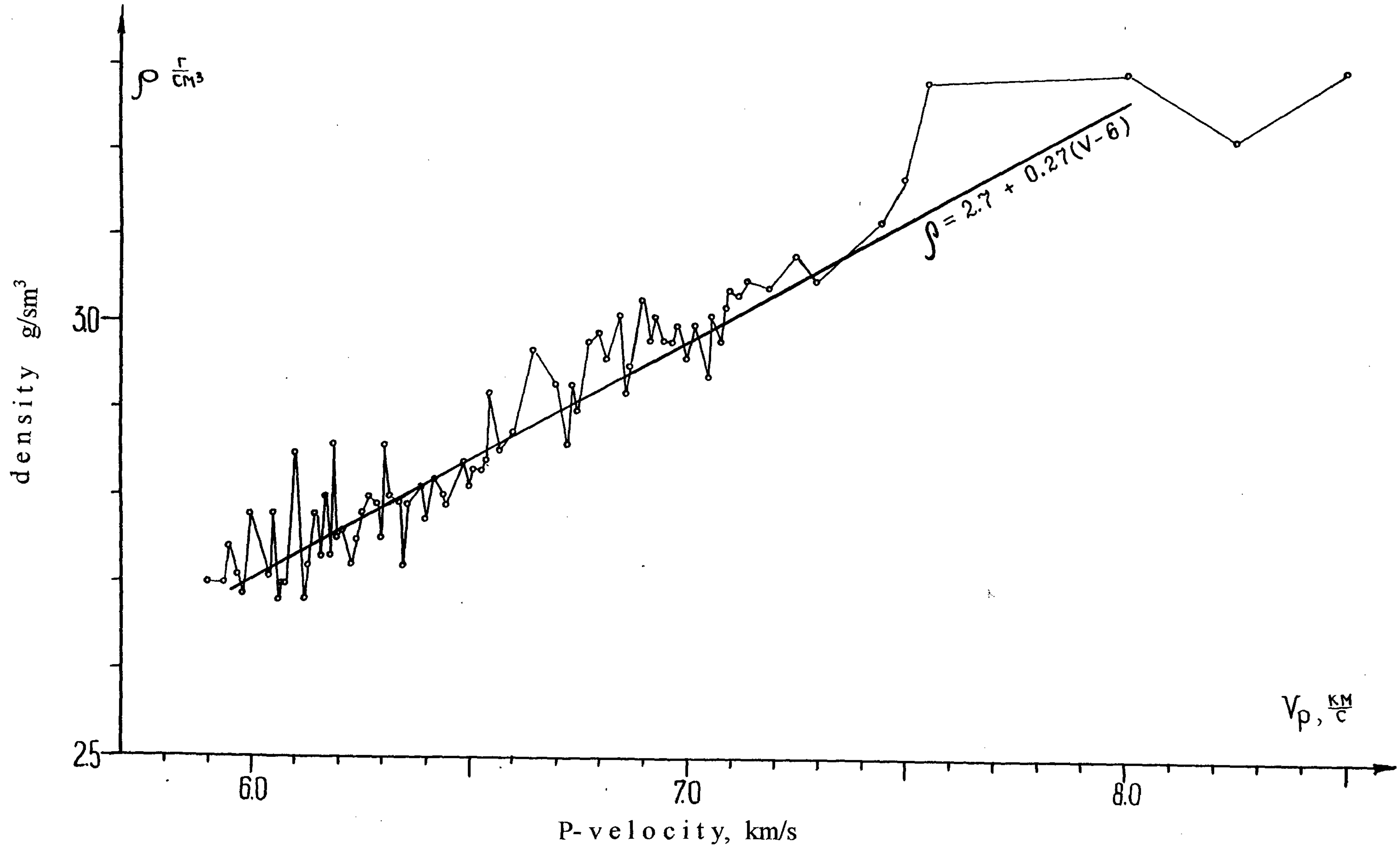

$\rho\ \frac{г}{см^3}$
density g/sm^3
3.0
2.5
$\rho = 2.7 + 0.27(V-6)$
$V_p, \frac{км}{с}$
6.0
7.0
8.0
P-velocity, km/s

Fig. 26

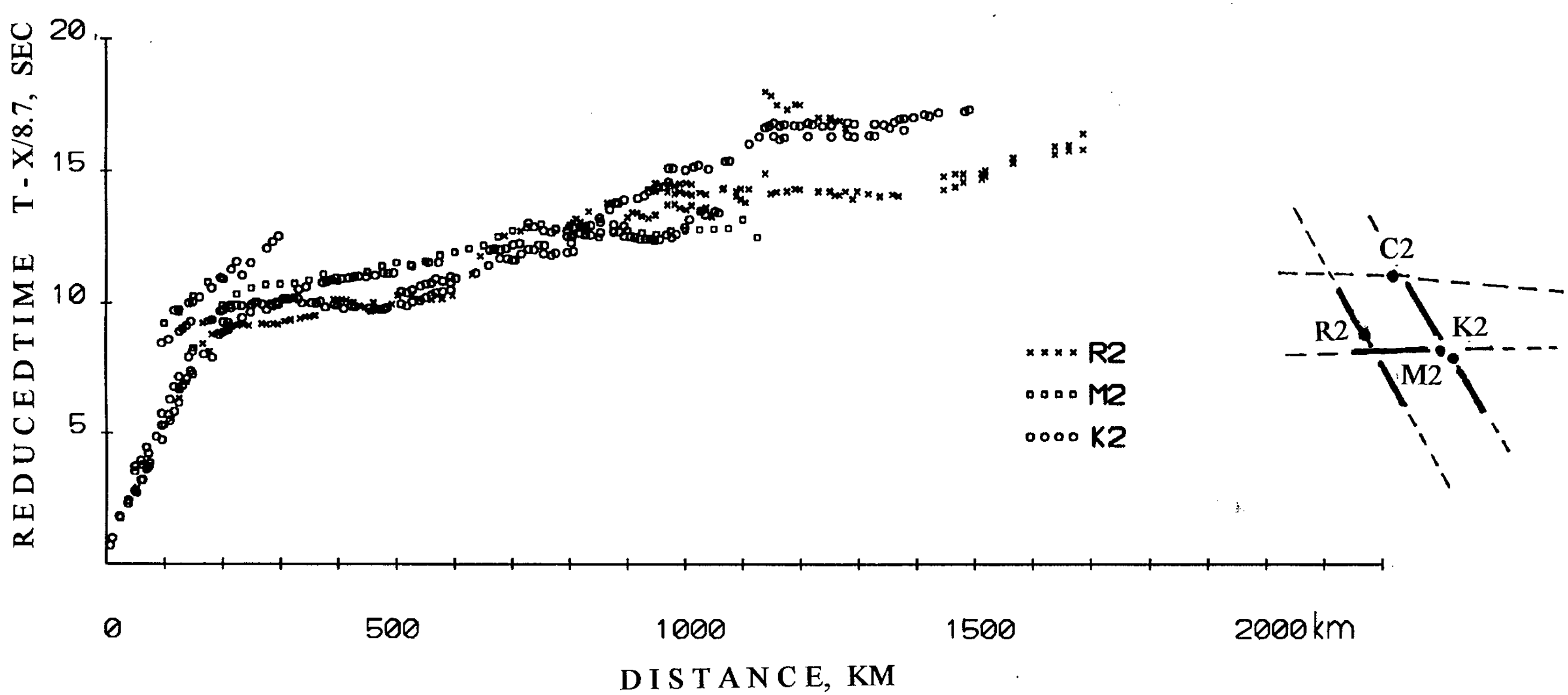

REDUCEDTIME T - X/8.7, SEC
20
15
10
5
0
500
1000
1500
2000km
DISTANCE, KM
R2
M2
K2
C2
R2
K2
M2

Fig. 27

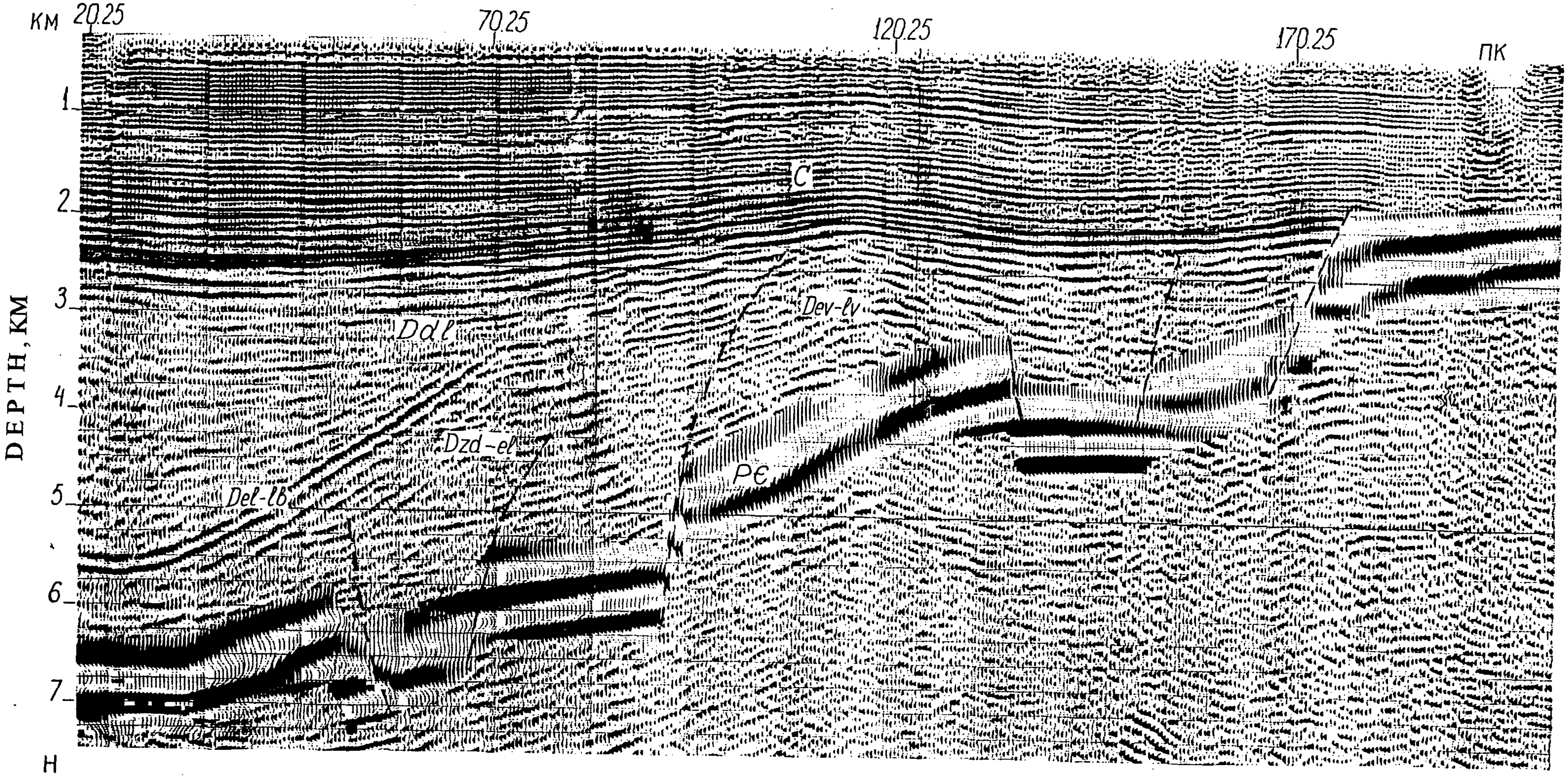
КМ
20.25
70.25
120.25
170.25
ПК
DEPTH, KM
1
2
3
4
5
6
7
H
C
Dev-lv
Ddl
Dzd-el
Del-lb
PЄ

Fig. 28

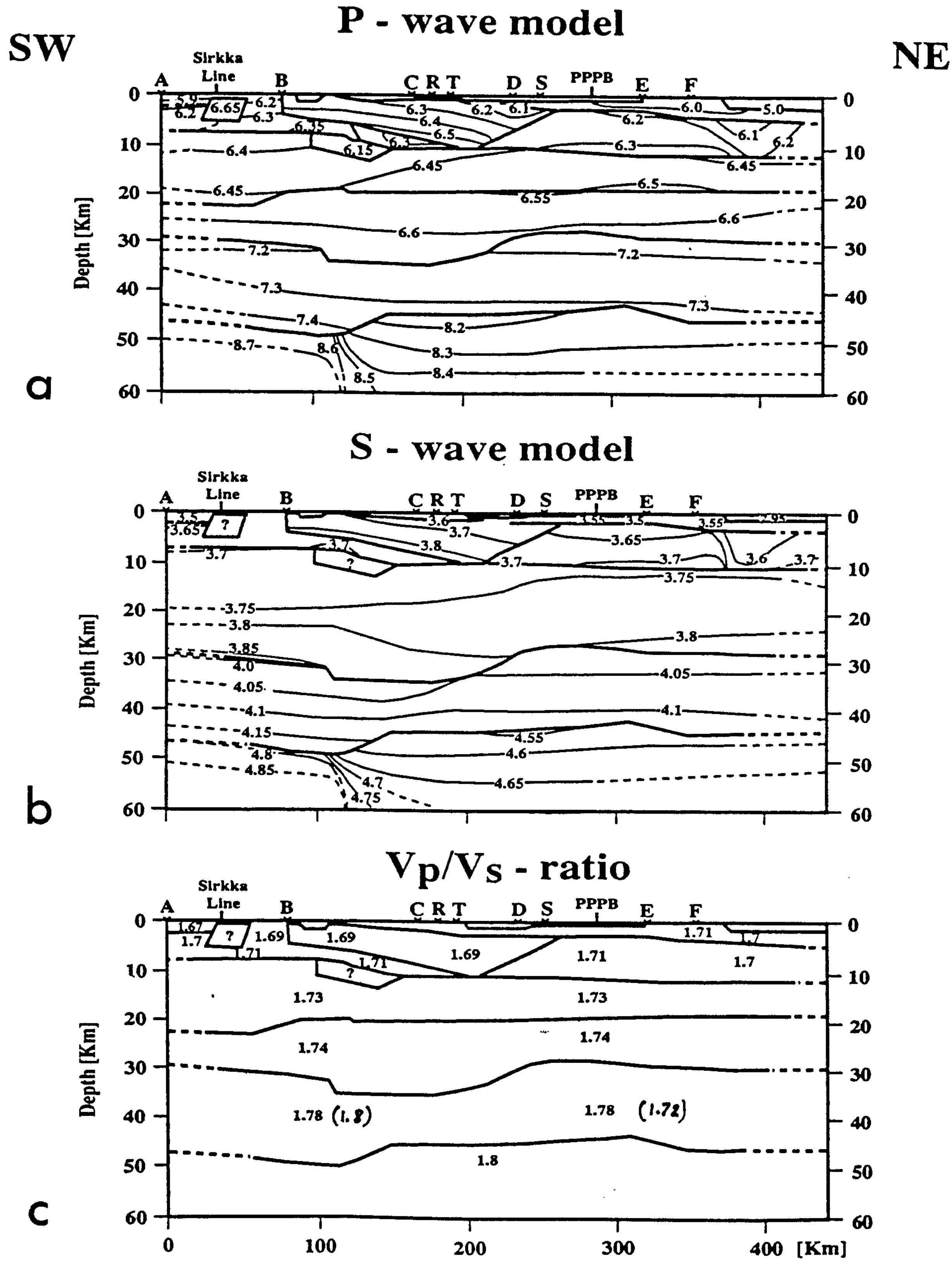
P - wave model
SW
NE
a
S - wave model
b
Vp/Vs - ratio
c
Sirkka Line
A
B
C R T
D S
PPPB
E
F
Depth [Km]
0
10
20
30
40
50
60
100
200
300
400 [Km]
1.69
1.71
1.7
1.73
1.74
1.78 (1.8)
1.78 (1.72)
1.8

Fig. 29

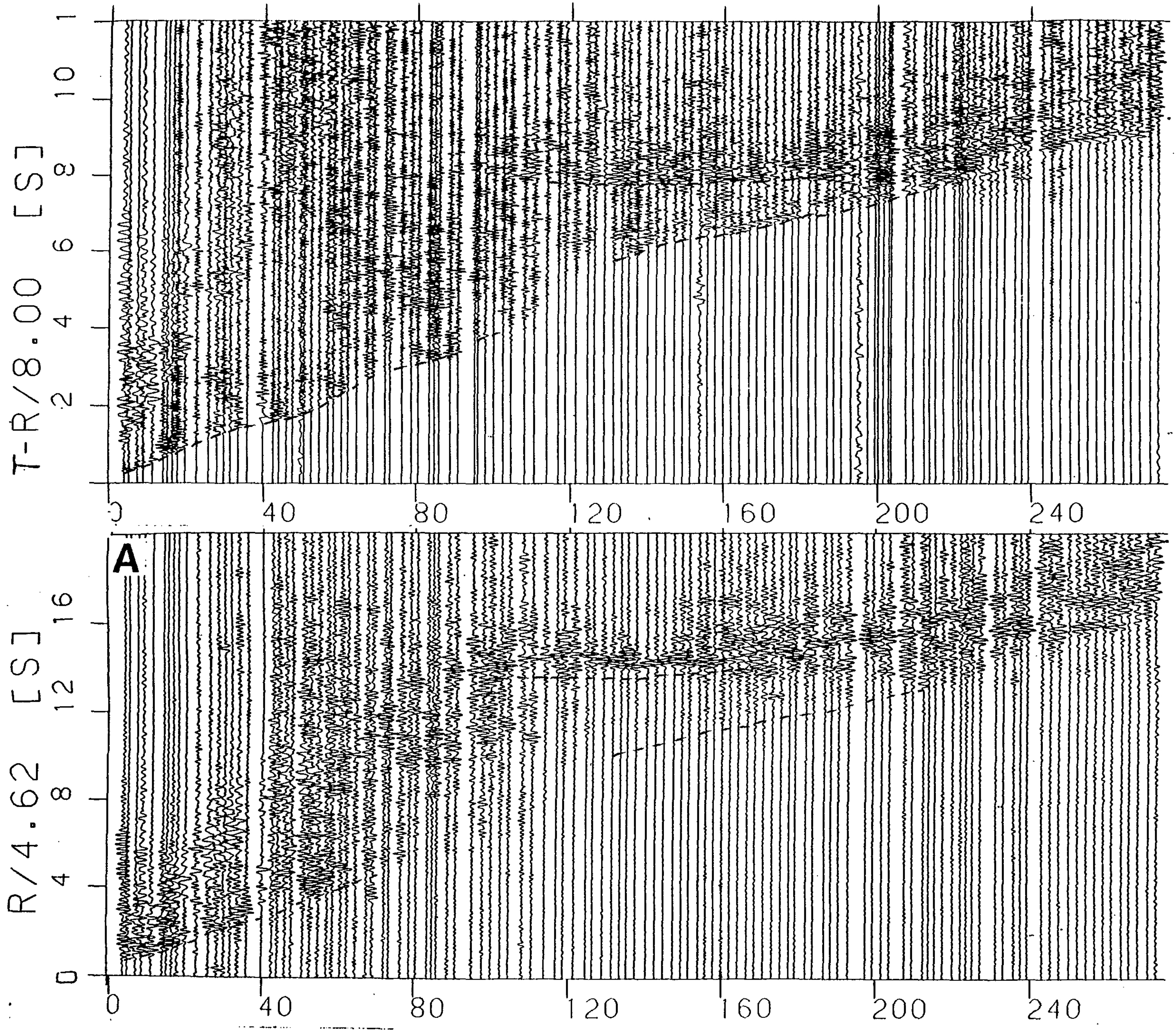

Fig.30

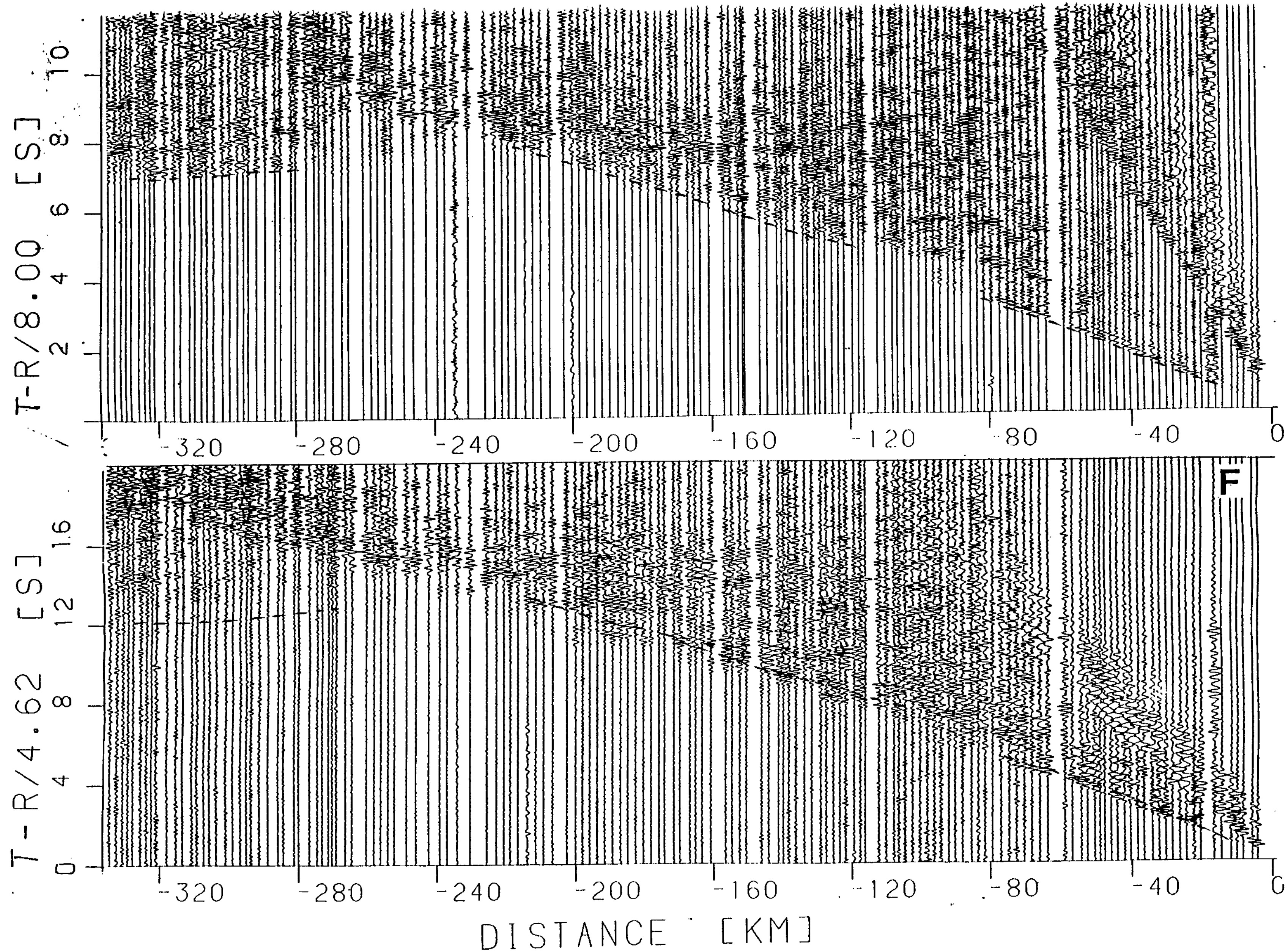
T-R/8.00 [S]
T-R/4.62 [S]
F
DISTANCE [KM]
0
-40
-80
-120
-160
-200
-240
-280
-320
2
4
6
8
10
12
16

Fig. 31

p-wave migrati

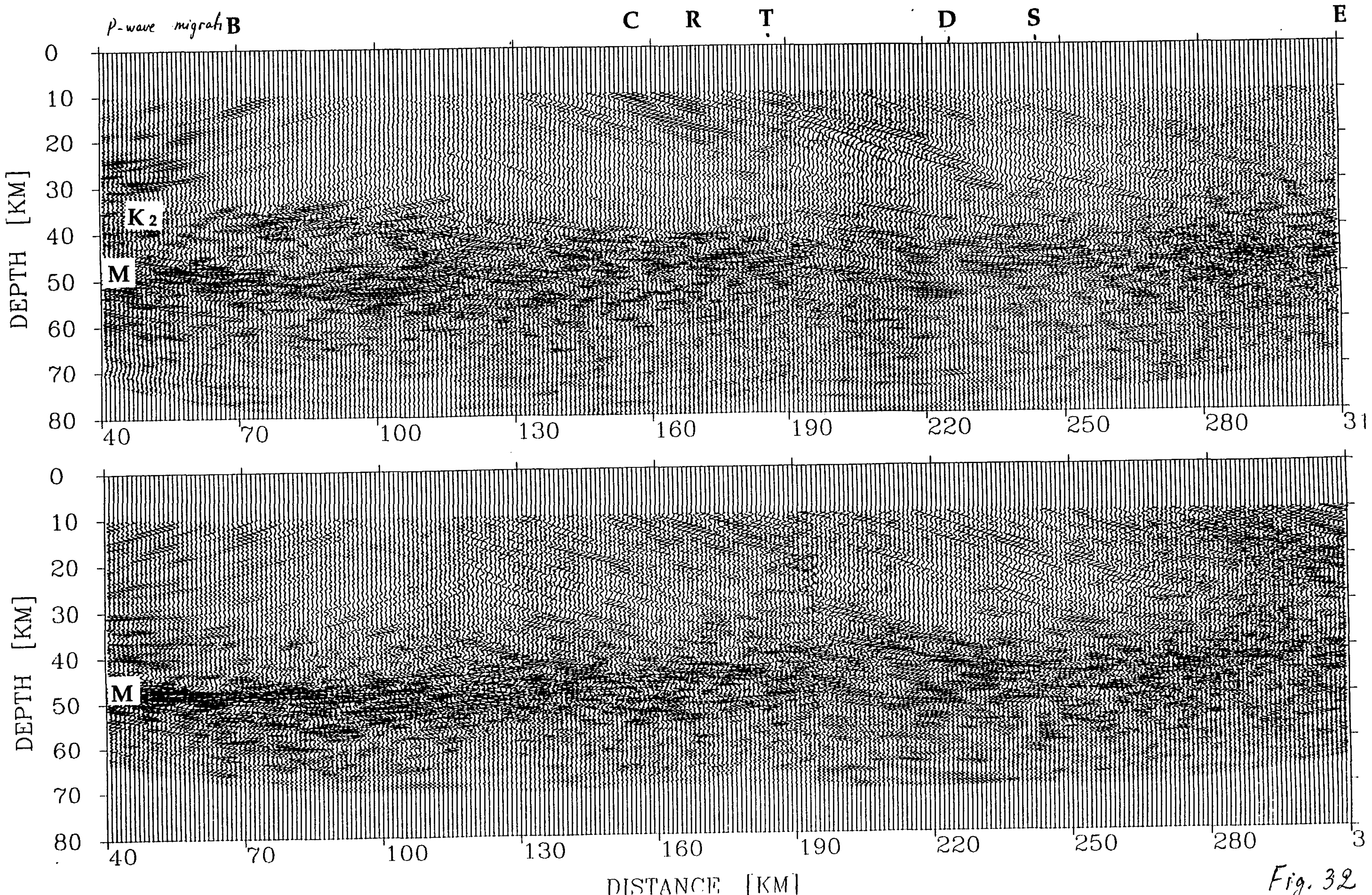

Fig. 32

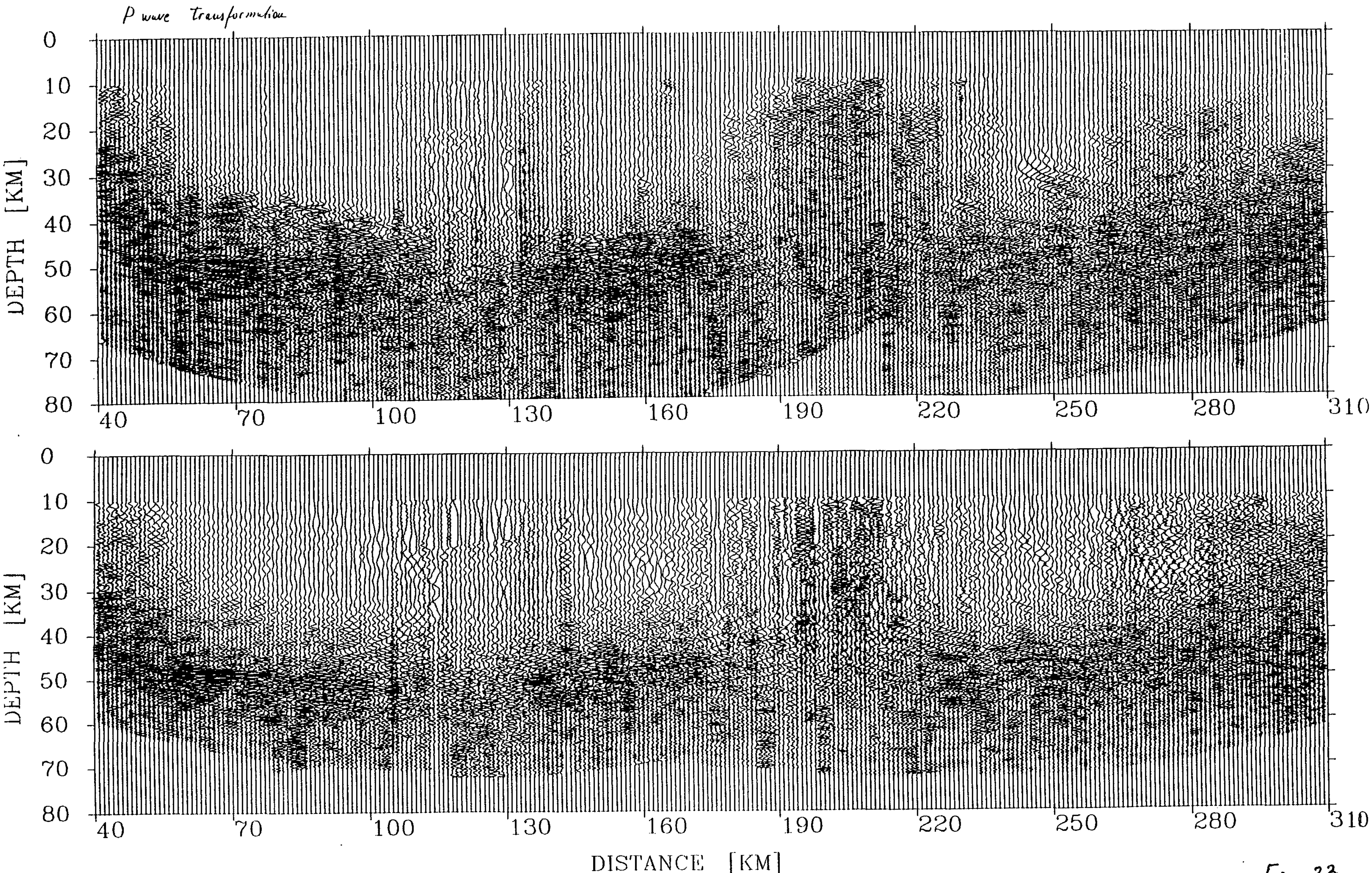
P wave transformation
DEPTH [KM]
0
10
20
30
40
50
60
70
80
40
70
100
130
160
190
220
250
280
310
DEPTH [KM]
0
10
20
30
40
50
60
70
80
40
70
100
130
160
190
220
250
280
310
DISTANCE [KM]

Fig. 33